USING LAND SURFACE MODELING TO EXPLORE THE INFLUENCE OF SOIL MOISTURE ON SEEDLING RECOVERY AFTER WILDFIRE

By

Eric Samuel Gordon

B.A., University of Pennsylvania, 2001

M.S., University of Colorado Boulder, 2009

A thesis submitted to the

Faculty of the Graduate School of the

University of Colorado Boulder in partial fulfillment

of the requirements for the degree of

Master of Arts

Department of Ecology and Evolutionary Biology

2016

This thesis entitled:
Using Land Surface Modeling to Explore the Influence of Soil Moisture on Seedling Recovery After Wildfire

written by Eric Samuel Gordon

has been approved for the Department of Ecology and Evolutionary Biology

____

Carol A. Wessman

____

Ben Livneh

Date_______________

The final copy of this thesis has been examined by the signatories, and we find that both the content and the form meet acceptable presentation standards of scholarly work in the above mentioned discipline.

Abstract

Gordon, Eric S. (M.A., Ecology and Evolutionary Biology)

Using Land Surface Modeling to Explore the Influence of Soil Moisture on Seedling Recovery After Wildfire

Thesis directed by Professor Carol A. Wessman

Previous research shows that multiple co-located disturbances can lead to a variety of potential outcomes in terms of the recovery of conifer forests across high-elevation landscapes. Ecophysiology literature has demonstrated that soil moisture and vapor pressure deficit can be critical to the success of conifer seedlings. To explore the role that variation in soil moisture plays in potential forest regeneration after major disturbances, I combined a field study of seedling recovery after the 2012-2013 Fern Lake Fire in Rocky Mountain National Park, USA with a novel attempt to estimate plot-level soil moisture using the Variability Infiltration Capacity land surface model. Results demonstrated that land surface modeling is a useful technique for estimating soil moisture at scales greater than that of an individual plant and for mitigating the limitations of sparse field observations. In addition, kurtosis of modeled growing season soil moisture was shown to be predictive of seedling success. More research is needed to determine whether these results can be replicated in other contexts.

Acknowledgements

Funding for this research was provided by the Ecology and Evolutionary Biology Department at the University of Colorado Boulder. I am extremely grateful to Professor Carol A. Wessman, who provided countless hours of advice, review, and insight critical to putting this thesis together. In addition, Dr. Ben Livneh, Dr. William Bowman, and Dr. Katharine Suding gave me invaluable assistance as members of my thesis committee and pushed me to continue to draw more out of my research. I am indebted to staff at the Continental Divide Learning Center at Rocky Mountain National Park, especially Paul McLaughlin, Scott Esser, Kelly Stehman, and Isabel Ashton, who provided guidance and logistical support for work in the field. Setting up field sites and collecting data was only possible with the hard work of three excellent assistants, Ryan Martin, Troy Zwolinski, and Miles Brous. Finally, I am always grateful for the love and support of my wife, Celia, and my daughter, Adi.

CONTENTS

TABLES

FIGURES

CHAPTER 1

FIELD-MEASURED SOIL MOISTURE AS A PREDICTOR OF SEEDLING SUCCESS FOLLOWING WILDFIRE IN SUBALPINE FOREST IN ROCKY MOUNTAIN NATIONAL PARK, CO, USA

Introduction

Disturbances in subalpine forests

Subalpine spruce-fir forests are the highest-elevation and coldest forest type in the Southern Rocky Mountains. Disturbance history studies (e.g., Kulakowski et al., 2013) have shown that these forests are characterized by low-frequency disturbances such as stand-replacing wildfires, blowdowns, and bark beetle infestations. Field surveys (e.g., Pelz and Smith, 2012) and modeling studies (e.g., Buma and Wessman, 2012; Collins et al., 2012) demonstrate that these disturbances, alone or compounded, can have significant impacts on early and later successional forest conditions, potentially resulting in transitions to different species compositions or even to meadows. Less attention, however, has been paid to the mechanisms that potentially control early successional responses following disturbance, especially given the long return intervals in these ecosystems (Bigler et al., 2005). Understanding such mechanisms could help develop predictive tools useful for carbon modeling, restoration, or post-disturbance habitat conservation.

Subalpine forests in the Southern Rocky Mountains are found roughly above 2500 meters in elevation and are comprised largely of early-succession stands of lodgepole pine (*Pinus contorta*) with Engelmann spruce (*Picea engelmannii*) and subalpine fir (*Abies lasiocarpa*) dominating older stands. Limber pine (*Pinus flexilis*) is found on drier slopes (Peet, 1981), and quaking aspen (*Populus tremuloides*) is an early colonizer of disturbed areas. These forests are characterized by complex disturbance regimes, with the most common disturbances being high-severity wildfire, bark beetle infestation, and blowdown (Kulakowski et al., 2013; Peet, 1981). A number of different types of studies demonstrate that these disturbances can produce significant changes in long-term species composition and forest structure (e.g., Collins et al., 2011; Kulakowski et al., 2013; Pelz and Smith, 2012). Moreover, recent research indicates that multiple co-located disturbances occurring over a short period of time can produce compounding impacts on early and later successional forest conditions that would otherwise not be predicted based on the effects of single disturbances. For example, in the Routt National Forest in northern Colorado, Buma and Wessman (2012) observed reduced seedling establishment after fire occurring in blowdown when compared to fire occurring in live forest, which led to significant long-term changes in modeled vegetation structure and type after a century of growth. Working in the same region, Kulakowski et al. (2013) found reduced regeneration of conifers and initial dominance by quaking aspen after multiple disturbances.

Effects of soil moisture on survival of conifer seedlings

A sizable body of work has established that microclimate strongly affects plant survival and is in turn affected by land cover characteristics, especially vegetation (Aussenac, 2000). Soil moisture has been shown to play a critical role in decreasing vapor pressure deficit (which affects how much water seedlings need to take up for survival and growth) and moderating air temperatures in temperate and subalpine forest stands (Von Arx et al., 2013). Soil moisture and leaf area index appear to be partly coupled, although a threshold effect may result in limited effects of a sparse canopy on microclimate (Von Arx et al., 2013). At the margins of climatic suitability for many conifer species, growing season moisture plays a significant role in survival

(Castro, 2016). Thus soil moisture may be particularly important to seedling success in subalpine stands, especially in challenging growing conditions such as the open canopy of a post-fire stand or in areas that experience significant summer drying.

Those findings, along with a general understanding of subalpine forest dynamics, provide reason to believe that conditions affecting the relative success of seedling establishment after disturbance may have a long-term impact on future forest composition, including the possibility of transitions away from conifer dominance. Trees are most sensitive to microsite conditions and resource availability during seedling establishment (Gray et al., 2005), with some seedlings dying within hours of germination under unfavorable conditions (Von Arx et al., 2013). Modeling analysis of a disturbed subalpine forest suggests that early seedling establishment can determine longer-term forest structure and composition (Buma and Wessman, 2012), and compounding impacts of multiple disturbances can create conditions favorable to species that reproduce vegetatively, such as quaking aspen (Kulakowski et al., 2013). Studies of undisturbed sites indicate that seedling establishment may be limited by soil temperatures and light availability (Lajzerowicz et al., 2004) or by canopy density and its consequent effects on site-specific water availability (Von Arx et al., 2013). In a study of mixed-conifer plots in the Sierra Nevada Mountains, Gray et al. (2005) found a positive relationship between soil moisture and frequency of most tree species, suggesting that lack of soil moisture may limit regeneration.

One potentially critical determining factor in seedling success following disturbances is availability of moisture in the seedling root zone (roughly the top 10cm of soil). Because available soil moisture is determined by a number of other site-specific factors, such as soil texture, soil organic matter, bulk density, litter depth, and climate (Brady, 1974), it can be considered an integration of a number of microsite factors. Existing work has indeed demonstrated that, along with vapor pressure deficit, soil moisture is a critical factor affecting the survival of individual seedlings (Gray et al., 2005; Von Arx et al., 2013). Moreover, among all disturbances, wildfire is particularly likely to affect soils in a manner that often reduces soil moisture (Ubeda and Outeiro, 2009), especially at seedling root depth (Gray et al., 2005). There is thus good reason to consider the possibility that availability of soil moisture in the seedling root zone could be a good predictor of the success of conifer regeneration following high-severity fire.

Although soil moisture is a complex variable affected by a number of site-specific conditions, its effect on seedling success can be better illuminated when other important parameters are relatively similar across sites. The ecophysiology research referenced above provides sufficient background to hypothesize that the ability of soil to hold plant available water in the seedling root zone is an important determinant of conifer seedling success in early (<5 years) recovery from wildfire, and variations in root zone soil characteristics after wildfire will result in variations in soil moisture. In this study, I attempted to control for various other factors in order to isolate a potential connection between soil moisture and seedling success at the plot scale following a high-severity wildfire in a subalpine forest in northern Colorado, USA. Given that western North America has experienced an increase in the frequency and acreage of forest fires and that such an increase is projected to continue as the climate warms (Dennison et al., 2014), understanding these relationships is increasingly important.

Conceptual model of seedling survival following wildfire

In order to determine how to control for factors other than soil moisture that could influence the success of tree seedlings, I developed a conceptual model of the factors necessary for seedling survival. The conceptual model shown here (Fig. 1.1) also illustrates potential confounding factors that could also influence seedling success.

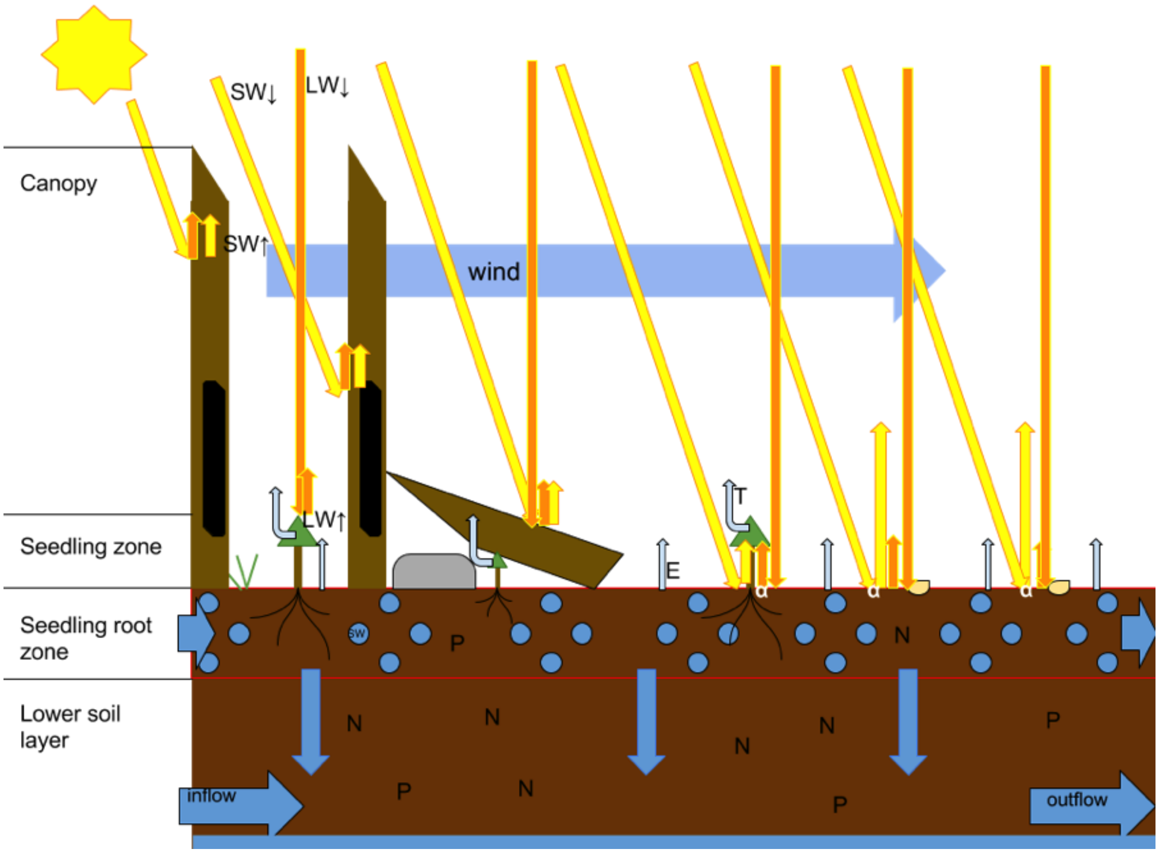

Figure 1.1. Conceptual model of factors affecting seedling success after wildfire in subalpine forests. Blue dots and arrows represent water stored or moving though the soil. Abbreviations: N = nitrogen; P = phosphorous; E = evaporation from soil surface; T = transpiration; SW↓ = incoming shortwave radiation; SW↑ = outgoing shortwave radiation; LW↑ = outgoing longwave radiation; LW↓ = incoming longwave radiation; α = surface albedo.

In this model, "seedling success" is defined as the survival of live conifer seedlings at a given site measured at a given time after wildfire. Following such a disturbance, any tree seedling needs the following (Oliver and Larson, 1990):

1. *Light* from the sun, which is represented as *SW↓* (incoming shortwave radiation).
2. *Water* obtained from the soil, represented by H_2O.
3. *Mineral nutrients* (N and P), also obtained from the soil, represented by $N+P$.

4. *Temperatures* in a suitable range, represented by *T*.

5. *Oxygen*, represented by O_2.

6. *Carbon dioxide*, represented by CO_2.

In addition, the presence of a seedling implies the availability of one or more seeds at the site in question and the availability of suitable surface on which to grow—for example, duff and litter can impede the germination of spruce seedlings (Knapp and Smith, 1982). Seed availability and surface conditions are represented jointly by *SS*. Thus we can describe a general equation for predicting seedling success:

$$S_{seedling} = f(SS, SW\downarrow, H_2O, N+P, T, O_2, CO_2) \text{ (Eq. 1)}$$

For seedlings on the soil surface, *oxygen* and *carbon dioxide* are not limiting factors, assuming a well-mixed near-surface atmosphere (a reasonable assumption in most real-world conditions). This allows us to simplify Eq. 1 into:

$$S_{seedling} = f(SS, SW\downarrow, H_2O, N+P, T, \cancel{O_2, CO_2}) \text{ (Eq. 2)}$$

Each factor in Eq. 2 is a product of a number of site-specific drivers that can be measured in the field or parameterized in a model. Thus we can specify these drivers for each factor:

1. Presence of a seed (assuming fire of sufficient severity to eliminate advanced regeneration) is a function of:

    a. State of existing seed bank (depends on pre-disturbance conditions and fire severity)

    b. Transport by wind (depends on prevailing wind direction, distance to seed source, condition of seed source, and stochastic factors); and

    c. Surface conditions (seeds cannot germinate on rocks or in water; conifer seedlings often struggle with too much duff/litter).

2. Availability of light for photosynthesis is a function of:

    a. Latitude

    b. Weather

    c. Time of year

    d. Aspect

    e. Ground cover (shading/non-shading)

    f. Albedo of soil (reflection up towards needles); and

    g. Microtopography.

3. Availability of water for seedling use is a function of:

    a. Initial soil moisture after snow melts (a function of snow accumulation and ablation)

    b. Precipitation during the growing season

    c. Matric potential, which is a function of soil texture

    d. Soil albedo, which affects evaporation from the soil surface and is a function of fire severity

    e. Ground cover, which affects shading to reduce evaporation as well as the competing influence of understory vegetation

    f. Bulk density, which determines porosity and thus the soil water holding capacity and is affected by fire severity

    g. Relative humidity, which determines vapor pressure deficit and thus the rate of transpiration by seedlings and competing plants; and

    h. Soil organic carbon and soil texture, both of which can affect the ability of the soil to hold moisture.

4. Availability of mineral nutrients is a function of:
    a. Soil type (parent material determines original nutrient content)
    b. Soil microorganisms to fix nitrogen
    c. Mycorrhizal fungi to break down inorganic phosphorous and aid in the uptake of plant-available nitrogen
    d. Age of soil and climatic conditions—weathering makes phosphorous available but too much weathering leaches out mineral nutrients
    e. Fire severity, which leads to breakdown or destruction of pre-fire organic matter; and
    f. Draining of soil, which is a function of soil texture and compaction after fire.
5. Optimal temperatures for growth are a function of:
    a. Air temperature
    b. Incoming shortwave radiation
    c. Soil albedo (influenced by fire severity)
    d. Ground cover (especially shading)
    e. Canopy cover (LAI'); and
    f. Soil moisture (partitioning of incoming energy into latent or sensible heat).

Although the above factors paint a complex picture of factors affecting seedling success, several major effects can be held constant in order to isolate the influence of soil moisture:

- Growing season precipitation
- Air temperature
- Incoming shortwave radiation at the canopy level
- Soil type

- Fire severity; and
- Surface conditions, including seed availability.

Thus by selecting plots with similar elevation, latitude, and aspect, one could minimize the influence of many of the most important confounding variables. Examining Eq. 2:

- Variability in availability of seeds can be controlled by setting a minimum distance from the nearest living tree. Soil surface conditions can be controlled by selecting only plots that experienced high-severity fire, which eliminates the organic layer.
- Incoming shortwave light is generally controlled given the same latitude and cloud cover if plots are close enough to the point that these factors vary imperceptibly across plots.
- Given the proximity of plots to one another, the availability of soil nutrients can be held roughly constant by similar soil type and texture.
- Air temperatures can be held constant given similar weather conditions and elevation.

Thus site selection can be used to control a number of variables (listed in Table 1.1) affecting seedling success, allowing us to isolate the influence of soil moisture, as described below.

Table 1.1. Variables derived from the conceptual model that are considered to be likely factors affecting seedling success after wildfire. Right-hand column lists means by which those variables can potentially be controlled to isolate the influence of available moisture.

Variable	Controlled By
Soil surface conditions	Selecting high-severity burn plots
Incoming shortwave light	Selecting high-severity burn plots and plots at the same latitude
Available moisture	*Variable of interest*
Available nutrients	Selecting plots with similar soil texture and type
Temperature range	Similar elevation and location

Methods

Study Area

The study area for this project was located in Rocky Mountain National Park (RMNP), roughly 100 kilometers northwest of Denver, Colorado, USA (see Figure 1.2). In 2012, a nearly nationwide severe drought (AghaKouchak et al., 2013) contributed to conditions ripe for wildfire, even at high elevations in the subalpine forest zone where fire return intervals often stretch for 200 years or more (Bigler et al., 2005). On October 9th of 2012, an illegal campfire on the eastern side of RMNP sparked a massive fire that climbed into a steep, inaccessible area in Fern Canyon. The resulting wildfire, known as the Fern Lake Fire, burned into the popular area of Moraine Park and consumed more than 3,500 acres of forest before it was officially declared out (US National Park Service, n.d.). Figure 1.3 shows an outline of the fire perimeter.

Figure 1.2. Location of Rocky Mountain National Park in the Rocky Mountains near Denver, Colorado, USA. Map by National Park Trips Media, http://www.myrockymountainpark.com/places/.

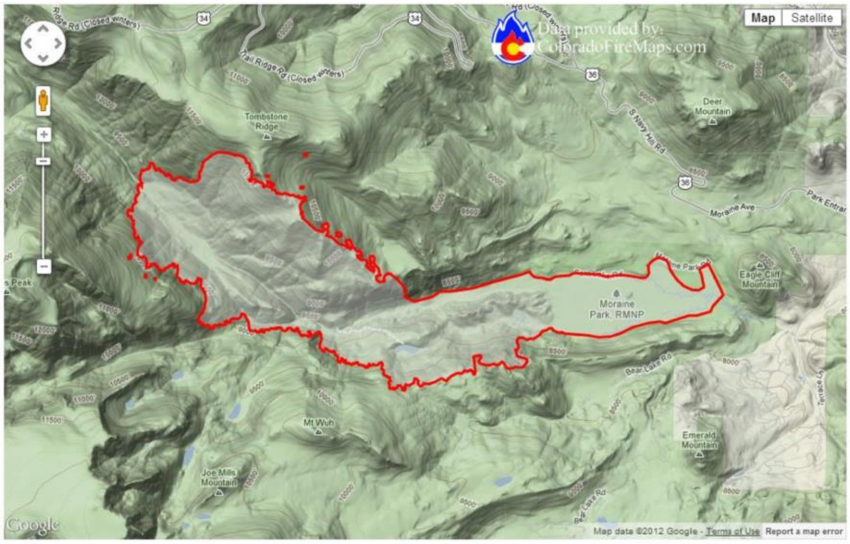

Figure 1.3. Perimeter of Fern Lake Fire in Rocky Mountain National Park. Data from COFireMaps.com, background image from Google Maps.

Elevations in the vicinity of the study area range from approximately 2500m to 3500m. At the lowest elevations in the Fern Lake Fire perimeter ponderosa pine (*Pinus ponderosae*) is common, but quickly transitions to a forest comprised of Douglas fir (*Pseudotsuga menzesii*) and lodgepole pine (*Pinus contorta*). Higher up, it then becomes a mixture of lodgepole pine, subalpine fir (*Abies lasiocarpa*), and Engelmann spruce (*Picea engelmannii*), as was the case within the study area and is common in subalpine forests along the Colorado Front Range. The forests found closest to treeline are generally comprised of only subalpine fir and Engelmann spruce. (Peet, 1981). Disturbance history is well-established in much of RMNP and indicates low-frequency fires at higher elevations along with large spruce beetle infestations and small-scale windthrow (e.g., Veblen et al., 1991).

Plot selection and setup

Selecting plots within the study area required controlling for a number of factors, as shown in Table 1.1. In order to control for the variable effects of climate, I first scouted and established three general sites roughly 1 kilometer apart and at similar elevations (approximately 2630m) and aspects (north-northeast). For consistency, plots were located in areas lacking young aspen. All plots were all in the vicinity of Cub Lake, a popular hiking area that provided relatively easy access on foot for our repeat sampling efforts (described below). Figure 1.4 is a satellite image of the three sites, all of which were divided into four plots.

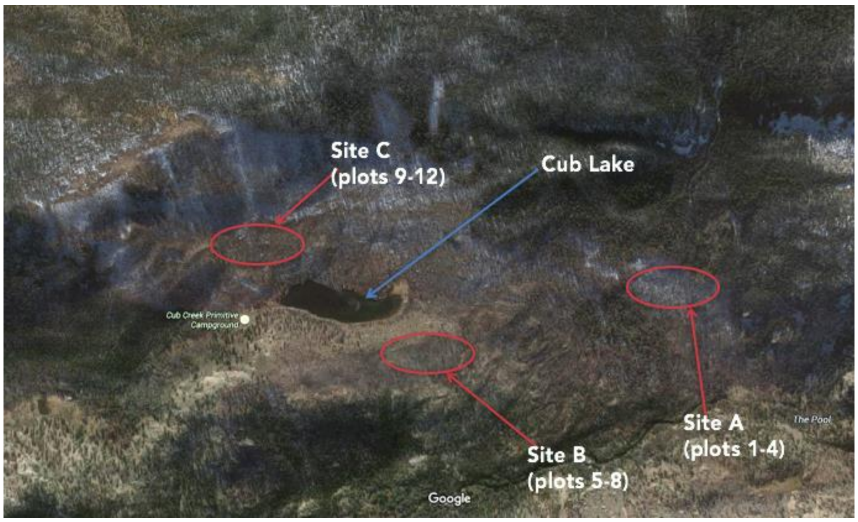

Figure 1.4. Satellite view of location of plots within study area. Background image from Google Maps, figure by author.

To ensure that all study plots represented high-severity wildfire, I checked the plot locations against the Relative Differenced Normalized Burn Ratio (RdNBR; Miller et al., 2009), a satellite-based imagery product developed by the US Geological Survey and US Forest Service for post-wildfire assessment. As shown in Figure 1.5, all of the plots I established were located within high-severity burn areas identified by the RdNBR imagery. In addition, an in-person survey of the ground conditions showed a lack of organic layer at all of the sites, indicating high-severity fire conditions.

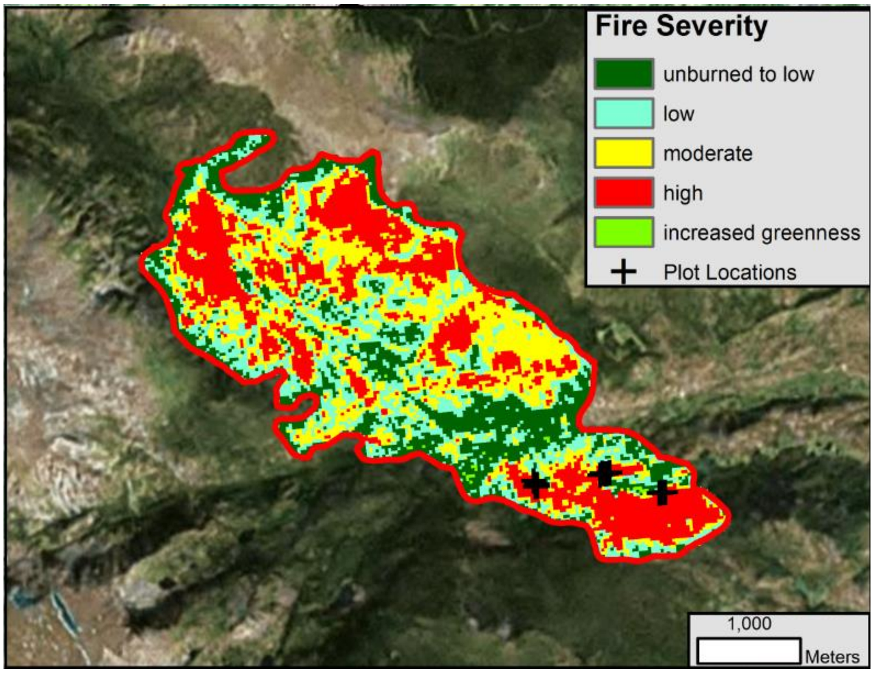

Figure 1.5. Severity of Fern Lake Fire burn area as estimated by RdNBR algorithm (Miller et al., 2009). Black crosses indicate study plot locations. Satellite image from Google Maps, figure by author.

Sampling design and data collection

At each site, four 15m x 15m plots were set up in early July 2015. Plot locations, elevations, and aspect were recorded using a handheld Garmin GPS unit (Table 1.2). Initial plot surveys included a census of all conifer seedlings (classified by species) located within the plot boundaries. Given that many of the conifer seedlings were less than 5cm in height, at least two people conducted seedling censuses to double-check that all seedlings were found and to increase the accuracy of each count. Diameter at 137cm height was measured for standing dead trees over 150cm tall. Heights of standing dead trees were estimated using a Haglofs digital clinometer.

Table 1.2. Number, location, elevation, and aspect of study plots. All plot locations are listed in UTM coordinates for plot centers, and are located in zone 13T. Aspect is reported as approximate compass direction orthogonal to downhill slope.

Plot Number	Easting	Northing	Elevation	Aspect	Slope
FL1	0444412	4466445	2620m	NW	1.6°
FL2	0444448	4466394	2625m	NW	12.8°
FL3	0444445	4466408	2640m	NW	16.2°
FL4	0444432	4466389	2636m	NW	21.7°
FL5	0445057	4466502	2663m	NW	17.1°
FL6	0445080	4466517	2665m	NW	16.4°
FL7	0445114	4466512	2664m	NW	19.0°
FL8	0445151	4466527	2664m	NW	19.1°
FL9	0445633	4466325	2655m	NW	13.5°
FL10	0445649	4466331	2655m	NW	8.2°
FL11	0445691	4466337	2655m	NW	11.25°
FL12	0445689	4466335	2655m	NW	9.0°

At each plot, ground cover was estimated visually. We placed a $1m^2$ quadrat divided into 25 square cells on top of the ground in the plot and estimated the percentage of each cover type within the quadrat. (Table 1.3 lists the cover types used in the study.) Given that ground cover was likely randomly distributed, this process was repeated in a regular checkerboard pattern across each plot, resulting in a total of 28 $1m^2$ estimations. Results were then averaged to provide an overall estimation of ground cover types per plot.

Table 1.3. Ground cover type categories used in visual estimation of ground cover at each plot.

Shrub
Forb
Grass
Coarse woody debris
Litter
Moss
Bare soil
Bare rock
P. tremuloides (aspen)
A. lasiocarpa (subalpine fir)
P. engelmannii (Engelmann spruce)

Permitting requirements from Rocky Mountain National Park limited the total amount of soil that could be removed from each plot and thus dictated part of our soil sampling protocol. We were able to take five individual soil samples from across each plot. Although we attempted to select random sampling locations, the rockiness of the soils throughout the study area constrained where it was feasible to remove soil. Samples were removed using a 10cm bulb corer, providing approximately 200 cm^3 of soil per sample. After removal, samples were double-bagged in Ziploc freezer-type bags to reduce moisture loss and transported in insulated containers back to a laboratory, where they were stored in a refrigerator at 2.8°C until they were used for analyses.

Soil samples were used to measure gravimetric water content at the time of sampling and to determine soil texture. Following standard methods, a portion of each sample was weighed with moisture, then oven-dried at 100°C for 24 hours and weighed again, and gravimetric water content was reported as percentage of water weight in each sample (Jarrell et al., 1999). A 2mm sieve was then used to remove any large rocks from the samples, and $40cm^3$ of the dried and sieved samples were weighed to determine bulk density. Gravimetric water content and bulk density measurements were averaged across the five samples to report a single figure for each plot.

To determine soil texture, we used a commonly-established mechanical analysis method (Elliott et al., 1999). 50 grams of oven-dried and sieved soil from each sample were added to 1 liter of distilled water with 5 milliliters of sodium hexametaphosphate, which helped avoid soil clumping. After mixing via a power blender for five minutes, the mixture was transferred to a graduated cylinder and hydrometer readings were taken at 40 seconds and 20 minutes. These readings were used to determine grams per liter of silt and clay as well as sand, allowing for soil texture to be determined by percentage of each separate. Silt, clay, and sand separates were averaged across all five samples to create an average soil texture for each plot.

Repeat soil moisture measurements were necessary to provide a picture of the change in soil moisture during the course of the growing season. Because additional soil samples were neither permitted nor feasible, we used a Hydrosense soil moisture probe (Campbell Scientific) with 12cm prongs to take 10 random soil moisture measurements per week at each plot. These readings were reported as volumetric water content (percentage of total soil volume comprised of water.) The Hydrosense probe (Figure 1.6) uses time domain reflectometry technology (see Jarrell et al., 1999), integrating the conductivity between two probe prongs to estimate the amount of moisture in the soil to the nearest whole percentage. At each point where the Hydrosense probe was used, soil temperature at 8cm depth was measured to the nearest 0.1°C.

Figure 1.6. Hydrosense soil moisture probe (Campbell Scientific) used for repeat sampling in this study. Probe uses time domain reflectometry technology to output volumetric soil water content as a percentage. Photo by Maja Krzic, University of British Columbia.

Results

Plot characteristics

Given that the plots were all located in areas that had experienced high-severity burn less than three years prior to the plot surveys, there was little living ground cover and little to no organic matter on the soil. However, there was a great deal of variation in the amount of bare rock at each plot, which would affect the ability of seeds to germinate and turn into viable seedlings. In addition, some plots showed more understory vegetation, primarily grass and forbs, while others were nearly bare. Figure 1.7 shows the distribution of ground cover types across each plot.

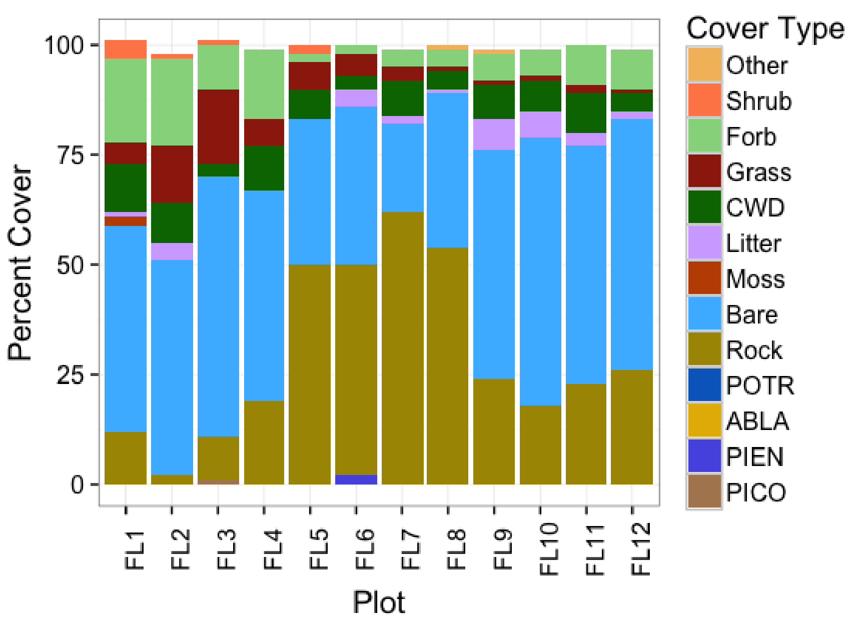

Figure 1.7. Percentage of each plot comprised of various ground cover types. CWD = Coarse Woody Debris; POTR = *P. tremuloides* (aspen); ABLA = *A. lasiocarpa* (subalpine fir); PIEN = *P. Engelmannii* (Engelmann spruce); PICO = *P. contorta* (lodgepole pine). Bars do not add up to 100% due to rounding.

Pre-fire forest density, as measured by the area of each plot comprised of standing dead tree stems (i.e., basal area), also varied considerably (Figure 1.8). Note that despite the severity of the fire, most of the burned trees were still standing at the time of the plot surveys.

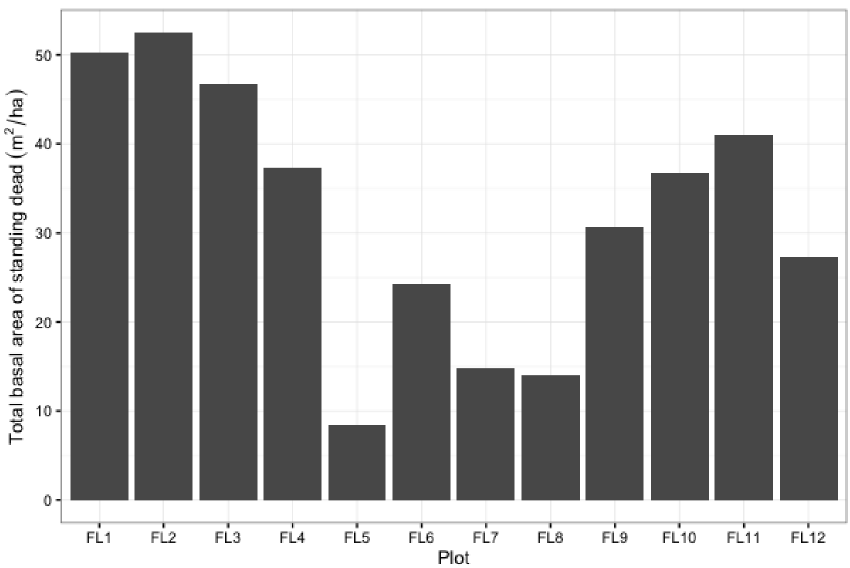

Figure 1.8. Basal area (area of plot covered by tree stems) of standing dead trees in each plot. Each bar represents total basal area.

Soil across the study area is primarily colluvium and till derived from granite, gneiss, or schist (Soil Survey Staff, Natural Resources Conservation Service, n.d.). Mechanical analysis of soil determined that all of the plots contained sandy loam soils (Figure 1.9), and texture varied relatively little across plots. Bulk density showed more variation, however, ranging from roughly 0.8 g/cm^3 to just over 1 g/cm^3 (Figure 1.10).

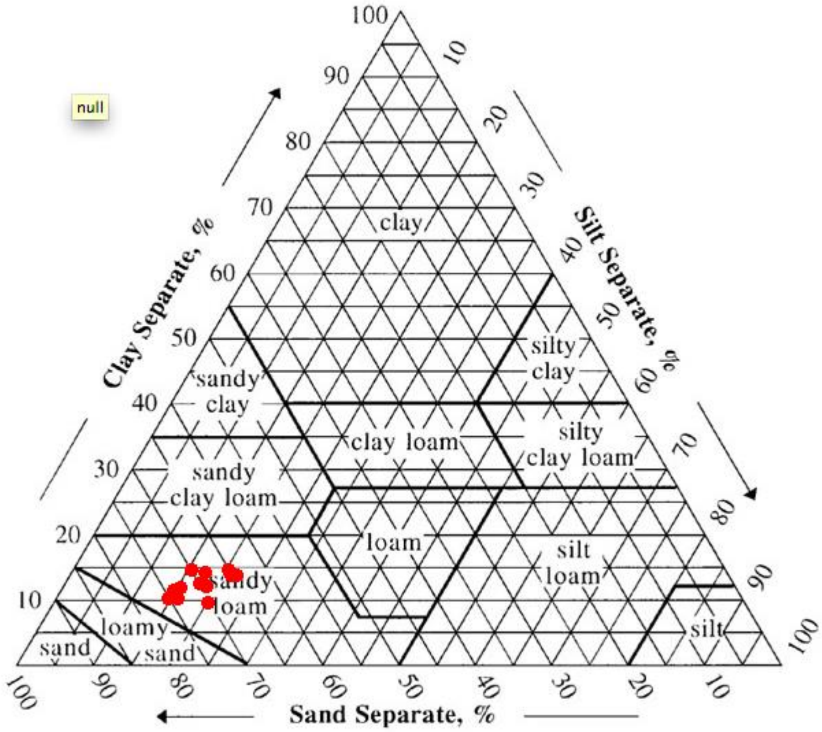

Figure 1.9. Average soil texture in study plots. Each red dot represents the texture of an individual plot averaged from five samples.

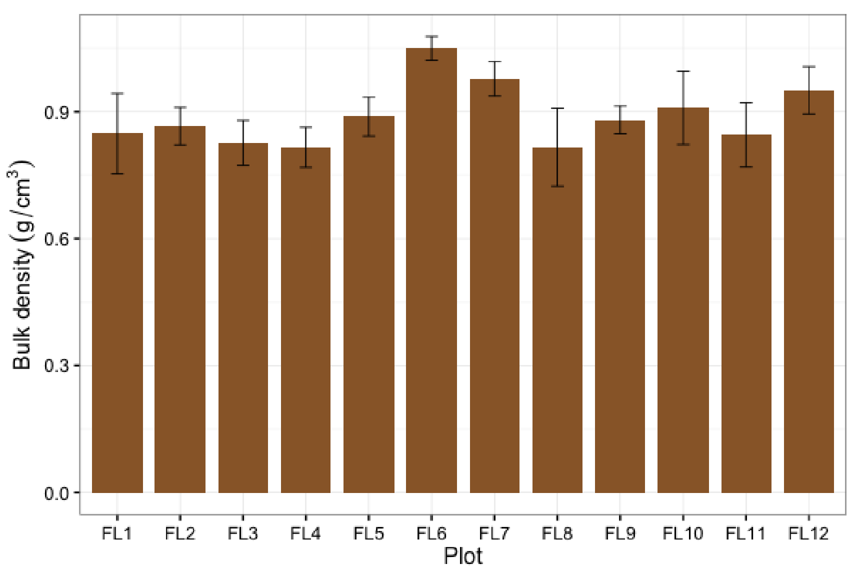

Figure 1.10. Bulk density of soil at each plot, based on five samples per plot.

Seedling counts

As described above, seedlings were counted individually across each plot and verified by at least two people. To the degree feasible, seedling species was identified as one of the three dominant conifer species in the study area (*P. contorta*, *P. engelmannii,* and *A. lasiocarpa*), although accurately determining species in seedlings can be difficult due to the lack of cones to use for identification. The vast majority of seedlings observed were first-year growth, as determined by the lack of whorls, although a few second-year lodgepole pine seedlings were found. Seedling density varied considerably across plots, as shown in Figure 1.11.

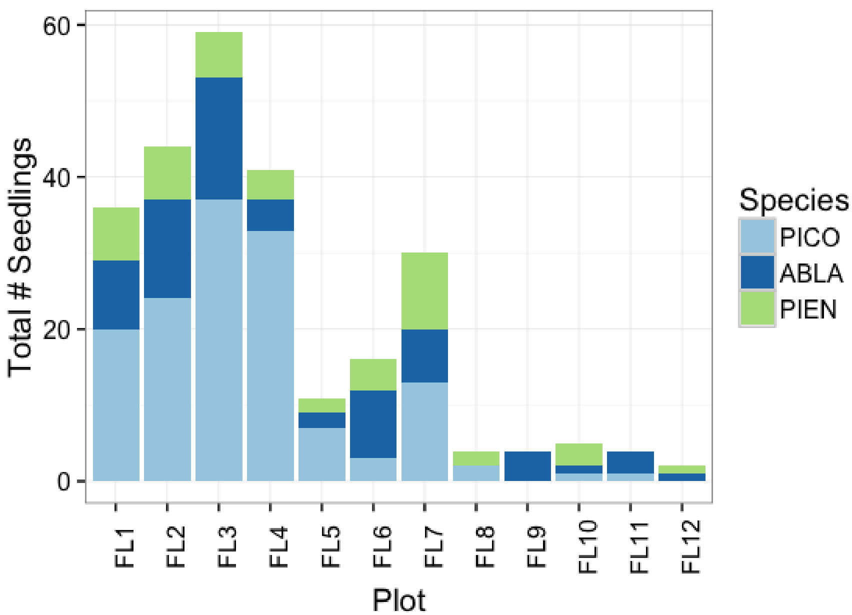

Figure 1.11. Total seedlings at each plot. Colors indicate species identified; PICO = *P. contorta* (lodgepole pine), ABLA = *A. lasiocarpa* (subalpine fir); PIEN = *Picea Engelmannii* (Engelmann spruce).

Because bare rock does not provide a suitable surface for seed germination and seedling growth, seedling counts were first converted into density (seedlings per hectare) and then adjusted for the percentage of each plot covered in rock (Table 1.4). All analyses of soil moisture and seedling density described in this thesis use adjusted seedling density.

Table 1.4. Seedling density at each of the study plots. Adjusted seedlings per hectare (far right column) represents density adjusted for the percentage of each respective plot covered in bare rock.

Plot	Total Seedlings	Seedlings/ha	% Rock Cover	Adjusted Seedlings/ha
FL1	36	1600.0	12%	1818.2
FL2	44	1955.6	2%	1995.5
FL3	59	2622.2	10%	2913.6
FL4	41	1822.2	19%	2249.7
FL5	11	488.9	50%	977.8
FL6	16	711.1	48%	1367.5
FL7	30	1333.3	62%	3508.8
FL8	4	177.8	54%	386.5
FL9	4	177.8	24%	233.9
FL10	5	222.2	18%	271.0
FL11	4	177.8	23%	230.9
FL12	2	88.9	26%	120.1

Soil moisture

Figure 1.12 provides an overview of the variation in soil moisture from gravimetric soil moisture measurements obtained from soil samples, a snapshot of the heterogeneity in soil moisture within each plot. Gravimetric water content measurements were converted into volumetric water content using the bulk density of each plot, allowing for the gravimetric data to be incorporated into a time series of volumetric water content. This allowed for all field measurements to be reported as percentage of soil comprised of water and the demonstration of change in soil moisture during the study period, which lasted from the beginning of July to the end of August 2015. The highest soil moisture levels in early July when there was abundant rainfall, with a general drying trend towards the end of the study period (Figure 1.13).

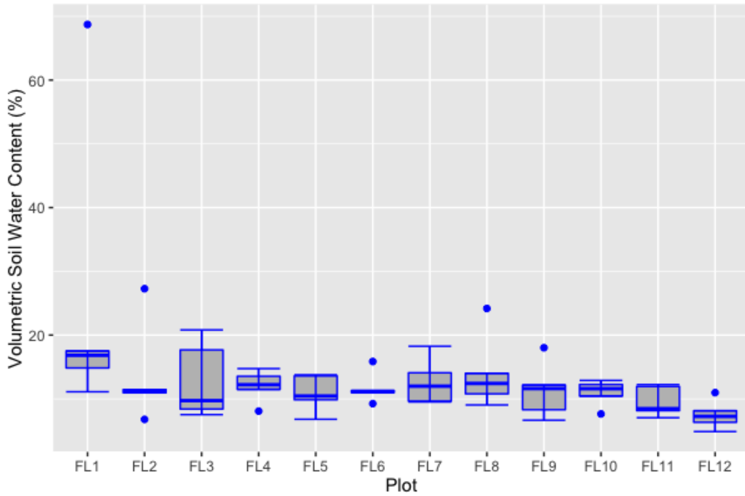

Figure 1.12. Boxplot of gravimetric soil moisture measurements obtained from five soil samples gathered from each plot in early July 2015. Values were converted to volumetric soil moisture using bulk density values.

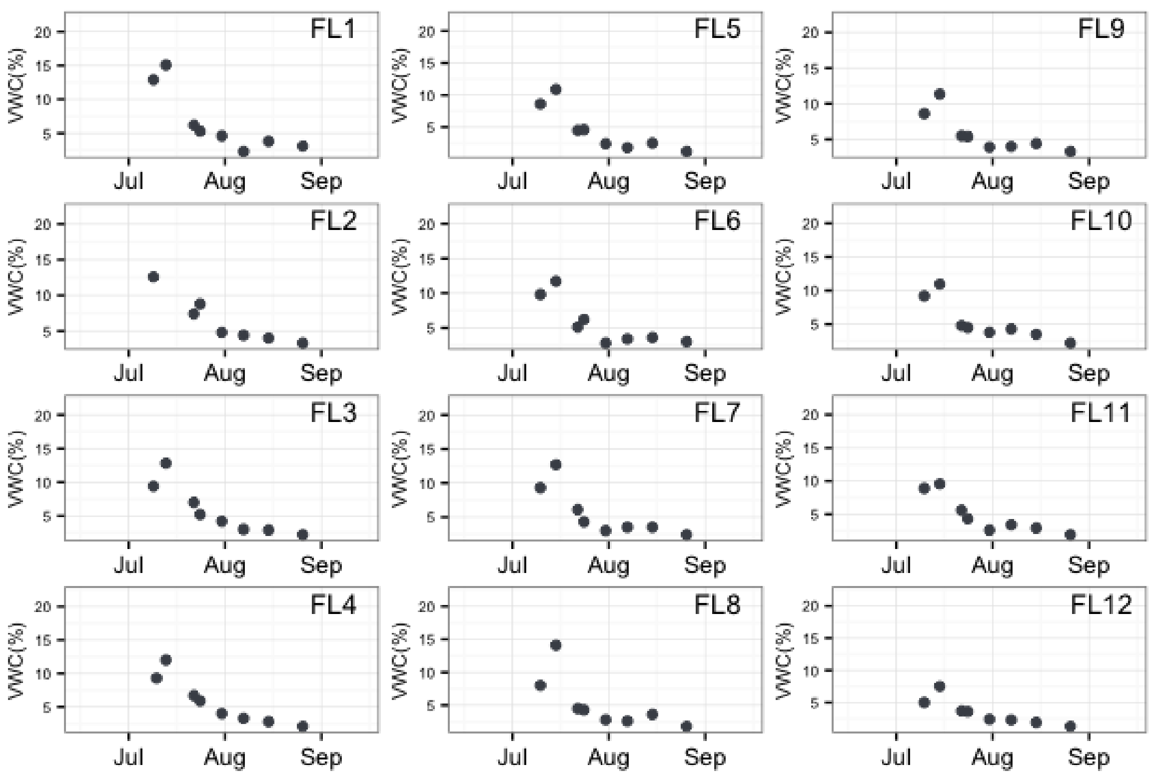

Figure 1.13. Volumetric water content estimates for each plot from weekly repeat sampling.

Analyses of predictors of seedling density

To assess the effect of soil moisture on the amount of seedling growth in each plot, I converted the time series of field-measured soil moisture into single data points. Neither the average of all field measurements of soil moisture (Figure 1.14) nor the total (not shown) were predictive of seedling density across the study plots. Finally, variability in soil moisture, as measured by coefficient of variation, was not predictive of seedling density (Figure 1.15).

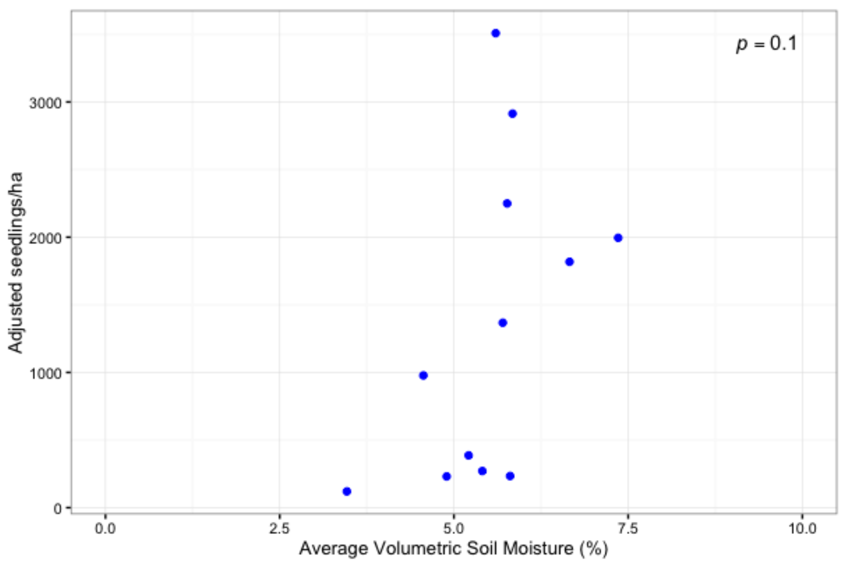

Figure 1.14. Scatterplot of average volumetric soil moisture values from repeat field sampling and adjusted seedling density at each study plot. P-value represents results of an attempted linear regression model.

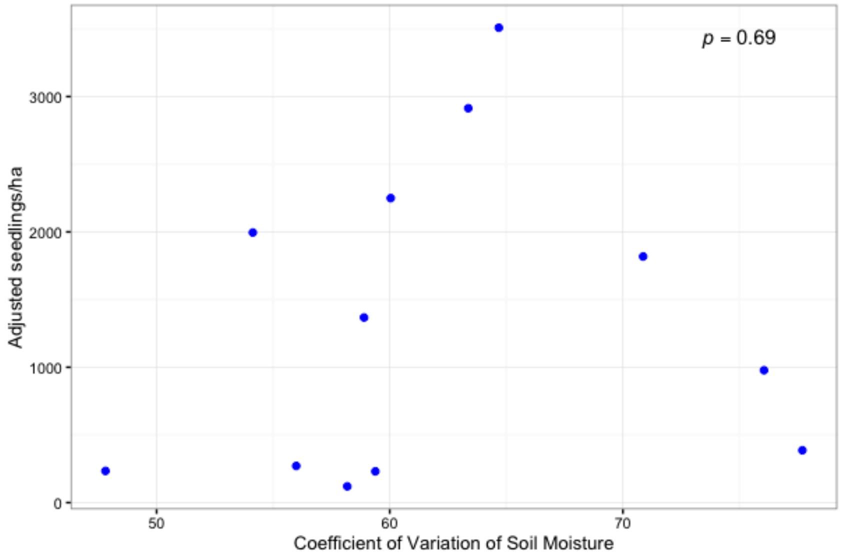

Figure 1.15. Scatterplot of coefficient of variation of soil moisture from repeat field sampling and seedling density at each study plot. P-value represents the results of an attempted linear regression.

Finally, I tested whether sheltering ground cover was predictive of seedling density. Previous research has demonstrated that sheltering cover on the surface, such as coarse woody debris, can moderate temperatures and provide more suitable growing conditions for conifer seedlings in some areas (Graham et al., 1994). Thus I combined the percentage of each plot estimated to contain grass, forbs, and coarse woody debris into a metric of "sheltering ground cover." The presence of such cover was not predictive of seedling density in the study plots, as shown in Figure 1.16.

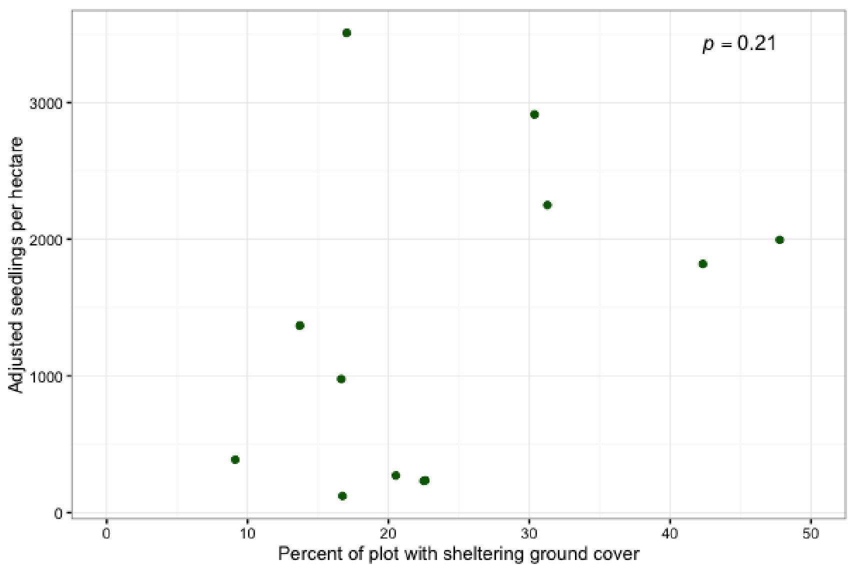

Figure 1.16. Scatterplot of percentage of "sheltering ground cover" (CWD, forb, and grass) and seedling density for each study plot. P-value represents the results of a linear regression.

Discussion

Overall, results show that field-measured soil moisture in the seedling root zone appears to be sensitive to summertime precipitation, even in an area where the bulk of the moisture falls as snow during the winter and spring. However, weekly manual measurements of soil moisture provided no ability to predict plot-level post-wildfire seedling density.

Soil moisture measurements taken at the 12 plots used in this study followed a predictable pattern in line with daily precipitation. Soil moisture was highest during the early portion of the month of July 2015, when a total of 56mm of rain fell during the first ten days of the month Soil moisture fell over the course of the summer in line with decreasing daily precipitation, as only 20.3mm of rain fell during the remainder of July and August (precipitation data from Bear Lake SNOTEL site, US Department of Agriculture Snow Survey.[1]) Thus there is good reason to believe that soil moisture as measured at 10cm depth by a Hydrosense time domain reflectometry probe is sensitive to summertime precipitation. Such a conclusion is quite

[1] http://wcc.sc.egov.usda.gov/nwcc/site?sitenum=322

relevant to seed germination and seedling viability, although snow accumulation and melt may be equally or more critical for more mature trees in subalpine forests.

Although the field moisture measurements were capable of demonstrating an overall pattern of change in moisture, metrics derived from the probe data had little variation and did not appear to be robust enough to use in larger-scale considerations of seedling success following wildfire in subalpine forests.

The lack of a clear relationship is likely due to the paucity of data. It is plausible that a relationship might appear in an analysis using more plots, but the primary issue appears to be the lack of variation in soil moisture measurements averaged or totaled across the growing season. One potential remedy to this lack of data could be the installation of soil moisture sensors connected to digital loggers that could take continuous data and provide much more information about the change in soil moisture over time. However, permit restrictions and lack of funding prevented such equipment from being used. In addition, part of the motivation behind this project was to explore more time and cost-efficient means of measuring soil moisture to allow for techniques to be scaled up for post-fire assessment of likely areas for seedling success.

Finally, it is important to note that this analysis did not account for potential threshold effects due to the lack of finer-resolution soil moisture data. Given their very small size, conifer seedlings may be vulnerable to minimum moisture values or extended periods with saturated soils. Conifer seedling mortality is generally very high during the first few years of life (Castro, 2016), and threshold effects may be responsible. The lack of soil moisture measurements at a sub-weekly time step may be hiding rapid changes in soil moisture that could have very real effects on the viability of individual seedlings. A much more elaborate field setup with logged soil moisture sensors placed in multiple study areas recorded over multiple growing seasons could provide more robust data to use in testing the original hypotheses. However, in the absence of a such a field campaign, in Chapter 2 I explore land surface modeling as a means to provide more soil moisture data for each plot.

CHAPTER 2

USING THE VARIABLE INFILTRATION CAPACITY LAND SURFACE MODEL TO EXPLORE THE EFFECTS OF WILDFIRE ON SOIL MOISTURE NECESSARY FOR POST-DISTURBANCE SEEDLING GROWTH

Introduction

The field of landscape ecology focuses on the heterogeneity of landscapes at a variety of scales and works towards improved representation of patterns and processes in heterogeneous contexts (Wu, 2013). There is no universally accepted means for representing such heterogeneity; rather, methods and types of analyses are tailored to the data available and the relevant research questions (Turner et al., 2011). Thus the field is continually evolving and searching for new ways to address a variety of challenges.

One such question facing landscape ecologists, ecohydrologists, and others is the accurate measurement of soil moisture at scales useful for landscape analyses and management applications. This question poses two challenges—the first being a technical one—the difficulty of obtaining accurate field measurements, especially in heterogenous non-agricultural soils (Jarrell et al., 1999). Although a number of techniques exist for rapidly estimating soil moisture, such as time domain reflectometry and installation of *in situ* soil tensiometers, these techniques all produce large errors when compared to careful laboratory measurements (Jarrell et al., 1999). The heterogeneity of forest soils, especially those in areas with younger soils and relatively low rates of weathering, adds an additional layer of complexity, making it virtually impossible to ensure truly accurate measurements at point scales.

More relevant to landscape ecology is the second challenge—trying to apply field measurements of soil moisture at individual points to scales relevant to landscape analyses. To estimate field moisture across a larger area, investigators generally combine multiple point measurements (Boone et al., 1999). In heterogeneous soils, especially with non-random distributions of land cover and soil characteristics, the question of "representativeness" of soil moisture measurements remains largely unanswered. Remote sensing techniques, such as those used to develop the recent Soil Moisture Active Passive (SMAP) satellite product (Entekhabi et al., 2010), can provide regional-level soil moisture estimates, but lack the resolution needed to work in mountainous terrain.

Thus in this study I turn to land surface modeling (LSM), which has frequently been used to estimate soil moisture in a number of hydrological and climatological analyses but has only begun to be used in some ecohydrologic applications (e.g., Livneh et al., 2015). I hypothesize that parameterizing a land surface model to create a continuous time series of soil moisture based on climatological data and soil parameters can provide useful estimates of soil moisture in mountainous, forested areas with heterogeneous soils. By using inputs based on soil, vegetation, and meteorological factors and calibrating to field measurements, LSM may be able to produce soil moisture estimates that are more representative of stand-scale conditions relevant to forest ecology questions than can be obtained by field measurements alone.

If the hypothesis related to LSM and soil moisture is supported, I can use model output to create a more robust picture of changes in moisture over time that can be used to investigate the influence of soil moisture on post-wildfire seedling establishment success in subalpine forests. Sparse field measurements, like those collected and analyzed in Chapter 1, provide only a broad overview of the changes in soil moisture that occur during the growing season when seedling viability sufficient for survival through the subsequent winter is established. Given the very high mortality rate among first-year conifer seedlings (Castro, 2016), subtle changes or threshold effects could be critical to survival. Generating a daily time series of soil moisture can support more detailed investigations of the relationship between change in soil moisture and seedling success. In addition to the greater temporal resolution provided by model output, LSM provides a stronger means for simulating the effects across a spatial area even when compared to continuously logged soil moisture sensors, which could provide similar temporal resolution but lack the ability to integrate conditions across a spatially explicit domain.

In this study, I investigate whether using LSM to estimate soil moisture during the growing season can provide novel insights into the role that soil moisture plays in seedling success after wildfires in the subalpine zone. This effort is explicitly exploratory; rather than trying to compile significant evidence supporting any conclusions about the relationship between soil moisture and seedling success, I gathered data sufficient to conduct a pilot study of the viability of LSM for efficiently estimating soil moisture in post-wildfire plots. I then used those soil moisture measurements to look into possible relationships between post-fire soil moisture and seedling success at scales greater than that of an individual plant to develop possible new avenues of research in post-disturbance forest ecology and ecohydrology.

Methods

Model Selection

A wide variety of land surface (alternately called "hydrologic") models have been developed for a wide variety of applications, many of which focus on enabling watershed-scale investigations of hydrology (Singh and Woolhiser, 2002). For this thesis, I selected the Variable Infiltration Capacity model (VIC; Liang et al., 1994) based on the availability of a course I could take that covered how to use the model as well as the available expertise of one of my thesis committee members (B. Livneh). VIC is a macro-scale, partially distributed model originally developed to allow for variability in land cover types within global climate simulations (Liang et al., 1994). During the more than 20 years since its initial development, however, it has primarily been used in hydrologic applications. In its most recent version, it incorporates two layers of vegetation varying in type over space and in leaf area index over time. Multiple layers of soil are simulated with varying infiltration capacities at multiple levels producing surface flow, baseflow, and groundwater recharge. Parameters for differential snow accumulation across elevation bands, full energy balance, and frozen surface lakes are available (see http://vic.readthedocs.io.) Figure 2.1 shows a generalized schematic of the VIC model.

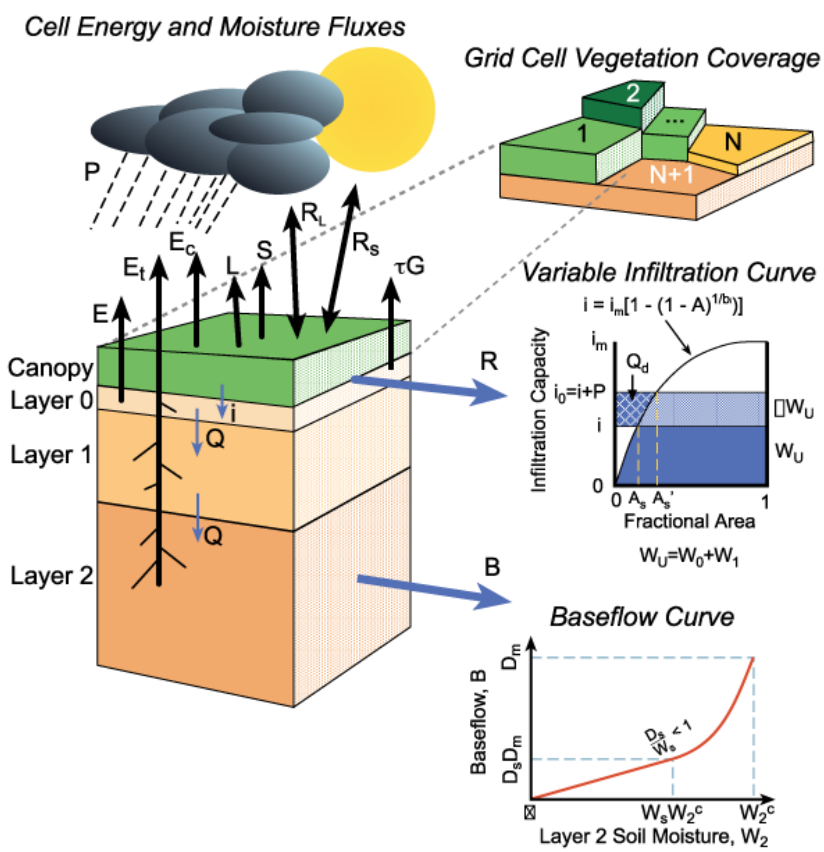

Figure 2.1. A generalized schematic of the Variable Infiltration Capacity land surface model. Image from vic.readthedocs.io.

The VIC model produces output for individual grid cells of uniform size. For runoff estimation and other large-scale hydrologic applications, a routing algorithm is added after the model has been run in order to estimate total water yield in the area of interest (see vic.readthedocs.io). However, in ecohydrologic applications, investigators will more likely be interested in energy and water balance terms affecting ecological parameters, for which the routing algorithm can be ignored. At this scale, it is often impractical or undesirable to vary infiltration capacity or other parameters across space; instead, investigators may wish to assume that a plot is effectively homogenous. For such an instance, spatial data can be removed from VIC inputs, and the model treats an entire cell as if it were a uniform point. Although this removes some of the spatial heterogeneity in the real-world site being investigated, it provides for a much simpler and faster estimation of energy and water terms that can be applied to larger-scale analyses.

Study area and field investigation

As described in Chapter 1, the study area used in this analysis is located in Rocky Mountain National Park in Colorado, USA. The Fern Lake Fire, which burned from October 2012 to January 2013, provided an ideal location to place easily accessible study plots that could be visited repeatedly during the growing season to capture field estimates of the change in soil moisture over time and with varying weather conditions. I set up 12 study plots with similar elevations, aspects, and locations in order to control for a variety of factors that could influence seedling growth (see Figs. 1.2-1.5 and Table 1.2 for more information regarding the study area and plot locations.) At each plot, relevant location and soil characteristics were collected for use in parameterizing the VIC model for each plot. Seedlings were counted manually and adjusted for percentage of bare rock in each study plot, creating a response variable to test against modeled soil moisture output. In addition, soil moisture measurements were taken weekly in July and August, with 10 random measurements of volumetric water content obtained at each plot using a Hydrosense soil moisture probe (Campbell Scientific).

Model parameterization

Table 2.1 lists parameters in the VIC model that were adjusted for analyses conducted in this study. The VIC model includes a large number of other potential user-defined parameters; for a complete list, see http://vic.readthedocs.io/en/vic.4.2.c/Documentation/Inputs/.

Table 2.1. VIC model parameters adjusted in this study.

Parameter	Units	Adjustments
SITE PARAMETERS		
Location	Lat/lon	Set to plot center as measured in the field
Elevation	m	Set to plot elevation as measured in the field
Start date		Estimated as date of snowmelt at each plot (see details in text)
End date		Date of first snowfall recorded at Bear Lake SNOTEL site (identical for all plots)
SOIL PARAMETERS		
Depth of top soil layer	m	Set to 12cm for all plots to match length of Hydrosense field probe
Bulk density, which affects porosity and thus water holding capacity of soil	g/cm^3	Set to value measured from average of five soil samples taken at each plot
Initial soil moisture	mm	Estimated based on bulk density
VEGETATION PARAMETERS		
Overstory leaf area index	m^2/m^2	Adjusted to represent relative differences in basal area of standing dead
Minimum incoming shortwave radiation for transpiration to occur	W/m^2	Set to 1200, an artificially high value that ensures no transpiration (appropriate to represent dead mature trees)
METEROLOGICAL PARAMETERS		
Daily maximum air temperature	°C	Bear Lake SNOTEL
Daily minimum air temperature	°C	Bear Lake SNOTEL
Incoming precipitation	mm	Bear Lake SNOTEL

Model inputs

To simplify analysis, the period for seed germination and seedling growth was limited to the snow-free season at each plot, creating a start and end date for VIC model runs. The start date was determined using remotely-sensed snow-covered area from the MODIS Snow-Covered Area and Grain size retrieval algorithm (MODSCAG; Painter et al., 2009). MODSCAG returns the fraction of each 500m resolution MODIS pixel that is covered by snow. This provides sufficient resolution to discern among some of the study area plots. However, because snow cover was inconsistent over the study area in late winter 2015, the beginning of the snow-free season was defined as the last date where fractional snow-covered area exceeded 25 percent for two consecutive days, including days where cloud coverage obscuring MODSCAG data preceded snow coverage. End date for all plots was set to the date when snow accumulation was first recorded at the nearby Bear Lake SNOTEL station (see below for details.)

Soil bulk density was estimated from soil samples taken during field surveys. Five samples were removed from each plot and sifted to remove rocks larger than 2mm. 40 cm^3 of each sample was weighed, and the resulting densities were averaged to create a single value for each plot (see Fig. 1.10). Soil porosity was then calculated using the formula:

$$\text{Total porosity} = [1 - (\text{bulk density}/\text{particle density})] \times 100 \quad \text{(Eq. 3)}$$

where particle density is held constant at 2.65 g/cm^3, a common assumption for mineral soils (Elliott et al., 1999). Porosity was then used to calculate initial soil moisture under the assumption that soils would be completely saturated upon snowmelt; thus initial moisture in millimeters was calculated as depth of the soil layer (12cm) multiplied by porosity. In addition, percentage of saturation, used in some metrics of soil moisture, was calculated as the value of soil moisture on a given day divided by initial soil moisture.

Vegetation parameters were adjusted in the model to represent the influence of standing dead trees in each plot. Transpiration was artificially turned off by setting the minimum level of incoming shortwave radiation necessary for transpiration to 1200 W/m^2, far above the 30 W/m^2 used for trees in most VIC model simulations (see http://vic.readthedocs.io/en/master/Documentation/Drivers/Classic/VegLib/.) To simulate the shading effect of standing dead trees in each plot, basal area measurements taken in the field were converted into measurements of LAI. Reference values were obtained from Pugh and Gordon (2013), who reported field-measured values of effective LAI (LAI') from stands of "grey phase" lodgepole pine (*P. contorta*) that had lost all needles and small twigs due to a bark beetle infestation. Variation in LAI at each plot was calculated by scaling the range of basal area values measured at each plot to the range of LAI' values reported in Pugh and Gordon (2013).

Finally, accurate growing season meteorological data was critical for this project, and proximity to a reliable climate station was incorporated into the selection of plot locations. The Bear Lake SNOTEL (Snow Telemetry; part of a network of remote snowpack measurement stations managed by the US Department of Agriculture's Snow Survey) station is located at 2900m, approximately 270m higher than the study plots and 3.6 km to the south (Figure 2.2; see also Figs. 1.3 and 1.5). The station instantaneously records snow-water equivalent during the snow season and precipitation during the growing season, along with air temperatures, and reports them in hourly and daily formats.[2] Daily maximum and minimum air temperatures and

[2] For more details on instrumentation and recordings taken at this station, visit the Bear Lake SNOTEL station web page at http://wcc.sc.egov.usda.gov/nwcc/site?sitenum=322.

daily precipitation from this station were used as meteorological inputs into all runs of the VIC model.

Figure 2.2. The Bear Lake SNOTEL site in Rocky Mountain National Park. Photo by author.

Results

Modeling soil moisture at study plots

The VIC model provides output for selected variables in tabular format. Thus I used the R software package (R Core Team, 2016) to create graphical plots and conduct statistical analyses on the model output.

To assess the quality of model outputs and compare to data obtained from the field study, I initially plotted soil moisture output as a time series for the modeled period, accompanied by a hyetograph of daily precipitation measured at the SNOTEL site. A brief inspection of the graphical output (see example in Figure 2.3) shows that soil moisture, as calculated by the VIC model for the 12cm-depth top layer of soil, rises and falls in a general pattern following daily precipitation. This demonstrates that the model is indeed capable of providing output that is responsive to daily weather conditions, at least within the geographic confines of the study area. Considering the precipitation pattern that occurred in the area during the summer of 2015, the soil moisture output seems reasonable—i.e., it stays quite high during the wet weather of July and drops much lower as the rest of the summer sees much less precipitation.

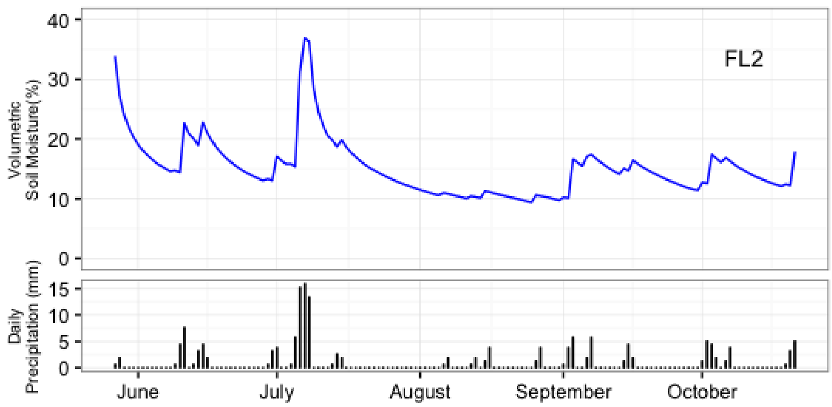

Figure 2.3. Example VIC model output of estimated volumetric soil moisture in the top 12 cm of soil (top graph) and accompanying daily precipitation data recorded at the Bear Lake SNOTEL station. This graph is for plot FL2 only.

I then compared model output to field measurements of soil moisture to assess the degree to which modeled soil moisture matched *in situ* data in terms of both magnitude and temporal pattern. These comparisons confirmed that model output did adequately represent the July peak in field-measured soil moisture and the subsequent drying. However, the magnitude of modeled soil moisture differed from field measurements, with the model producing roughly twice as much moisture as the field data showed (Figure 2.4). Adjusting bulk density allowed the model to more accurately reproduce field measurements (Figure 2.5). Doing so required increasing bulk density by a factor of 2, which resulted in bulk densities of nearly 2 g/cm^3, well above the range of 0.6 to 1.8 g/cm^3 typical for most soils (Elliott et al., 1999) and above the density permitting root penetration by most plants. A sensitivity analysis of the VIC model showed that modeled soil moisture is particularly sensitive to bulk density (see below.)

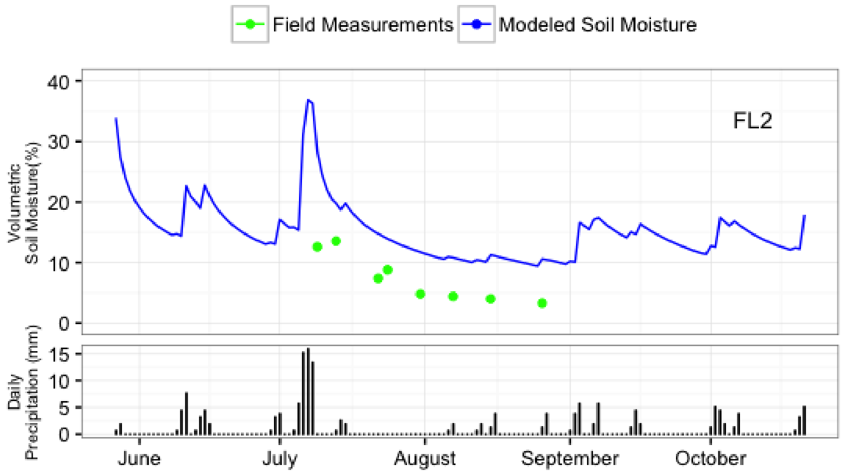

Figure 2.4. Same as Figure 2.3, but with weekly field measurements of soil moisture by Hydrosense probe added (green points.)

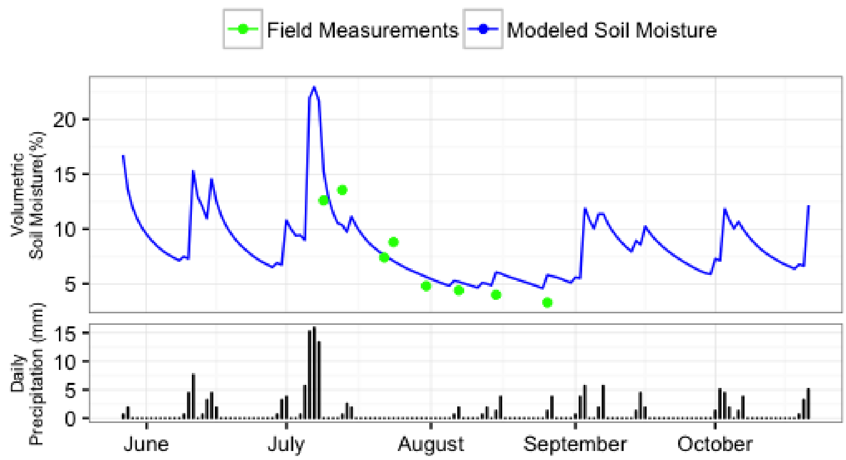

Figure 2.5. Same as Figure 2.4, but blue line represents VIC model output with bulk density at 200% of the parameter value in the original model run.

Increasing bulk density would have resulted in a closer fit between modeled soil moisture and field measurements. However, given that doing so would have required using unrealistic values of bulk density and that the study was aimed at assessing relative differences in soil moisture across plots rather than reproducing measured magnitude of soil moisture, I chose not to adjust the original modeled outputs. Moreover, there is no way to know whether the model or the field measurements are more accurate estimations of the “true” values. The probe used for taking field measurements relies on Time Domain Reflectometry, which assumes homogeneous, rock-free soils in the space between the two prongs of the probe. It is thus plausible that the model is as close to, if not closer to, the real-world values.

Figure 2.6 provides summary data in the form of boxplots of daily modeled soil moisture values at each of the plots. A one-way analysis of variance (ANOVA) indicates that there is a significant difference in soil moisture values across all of the plots ($p < 0.05$). Figure 2.7 provides modeled output with corresponding field measurements above hyetographs for all 12 of the study plots.

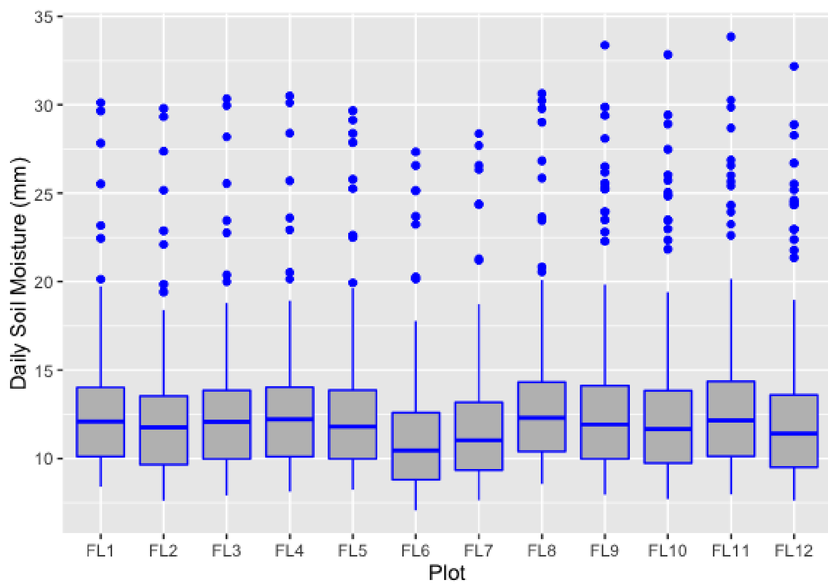

Figure 2.6. Boxplot of modeled daily soil moisture values at all of the Fern Lake field sites. A one-way ANOVA indicates a significant difference among the values of the means for each plot ($p = 0.003$).

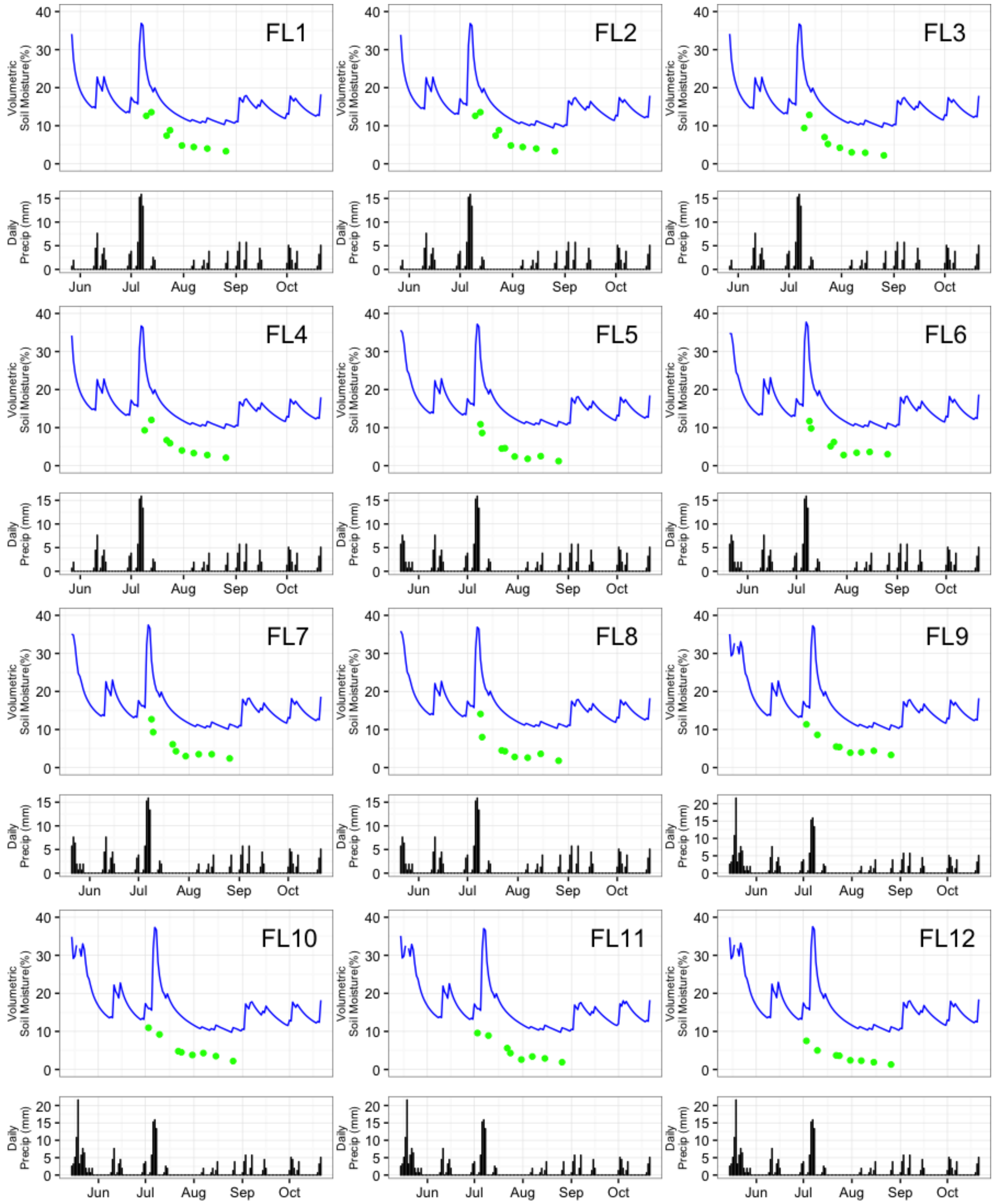

Figure 2.7. Modeled growing season soil moisture (blue line) with field measurements (green dots) for each of the 12 study plots. Each graph has an accompanying hyetograph below.

VIC model sensitivity

As mentioned above, soil bulk density appeared to have the strongest influence on soil moisture output in the VIC model. To better understand how the model responds to the bulk density of the soil, I performed a sensitivity analysis. Using output from the model run for plot FL2 (the same plot used in Figs. 2.3-2.5), I adjusted the bulk density parameter by increasing or decreasing it relative to the field-measured value. Increasing or decreasing bulk density by up to 20 percent of the field-measured value resulted in effectively no change, as shown in Fig. 2.8. However, soil moisture showed much greater sensitivity to greater changes in soil bulk density. A 50 percent reduction in bulk density resulted in higher soil moisture at all times with greater increases during drier periods. A 200 percent increase, on the other hand, resulted not only in much lower values overall but also much shorter peaks during wetter periods (Fig. 2.9). Future investigations of the use of the VIC model for soil moisture experiments may necessitate a consideration of how to adjust this parameter. Moreover, additional research is needed to determine whether it is feasible to better simulate rocky soils in the model, which could result in improved reproduction of field measurements of soil moisture in these types of conditions.

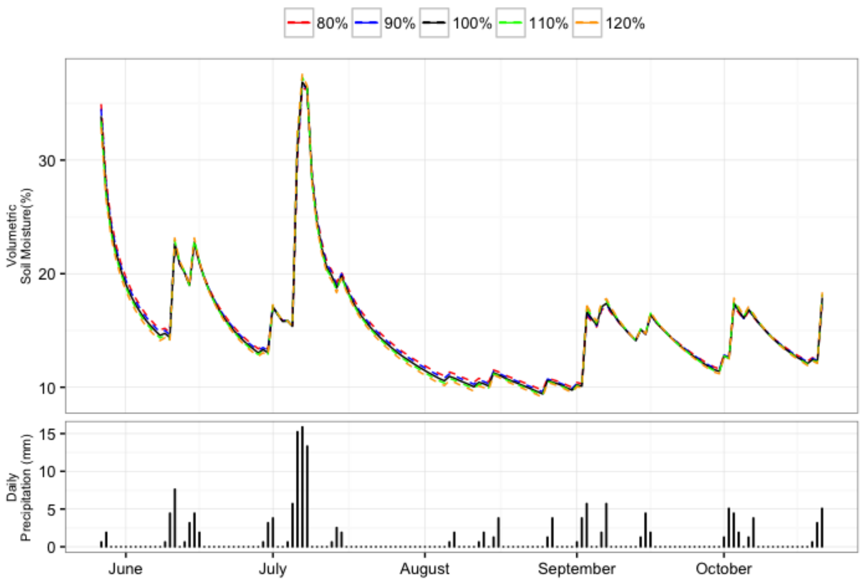

Figure 2.8. Sensitivity of VIC model soil moisture output for plot FL2 to bulk density. Colored lines represent bulk density set to different percentages of field-measured bulk density.

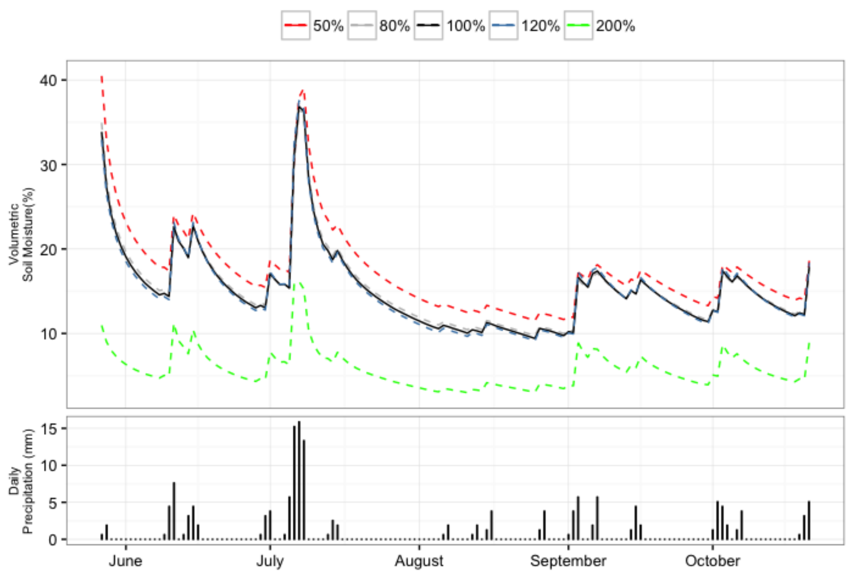

Figure 2.9. Same as Fig. 2.7, but with greater variations in bulk density.

Predictors of seedling density

Generating output from the VIC soil model produced a growing season-length time series of soil moisture for each of the study plots, at a daily time step. This is far more detail about soil moisture than was obtained via field measurements (see Chapter 1). A variety of analyses were performed using this these time series to explore whether various measures of soil moisture could have predictive relationships with the success of conifer seedlings in these post-wildfire areas.

Simple mathematical transformations of field-measured soil moisture data had not provided any predictive power for seedling density, as described in Chapter 1. However, the lack of any significant relationship could have been a result of the coarse temporal scale of data in the weekly sampling of soil moisture. Given that the VIC model output provides daily values, I was able to test whether greater temporal resolution might provide greater predictive power. Thus to provide direct comparisons to the analyses conducted with field data alone, I calculated simple mathematical averages, totals, and coefficients of variation for daily modeled growing season soil moisture at each plot. Figure 2.10 shows that total modeled growing season moisture, a metric of the maximum water available to seedlings in a given plot, has no predictive power for adjusted seedling density. Neither did the average daily value of soil moisture at each plot, as shown in Figure 2.11.

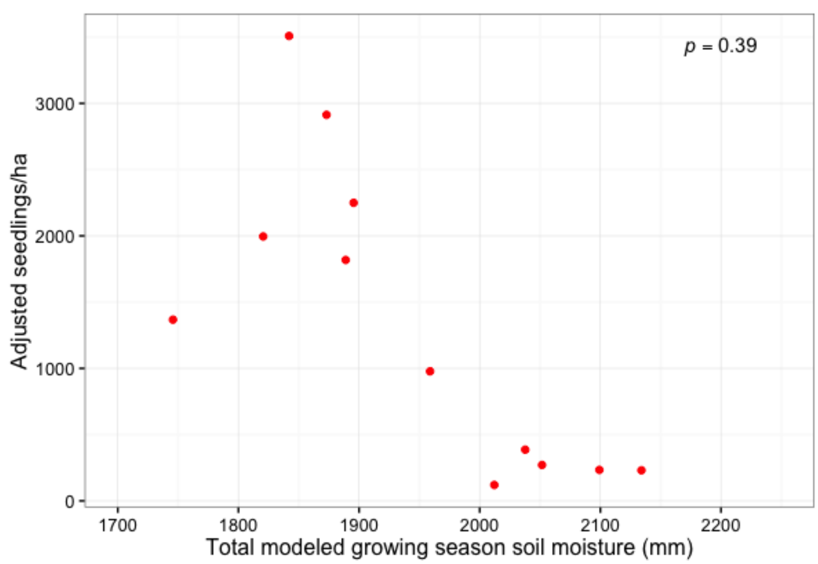

Figure 2.10. Seedling density as a function of the sum of growing season soil moisture values from VIC model output for each plot. P-value represents the result of an attempted linear regression.

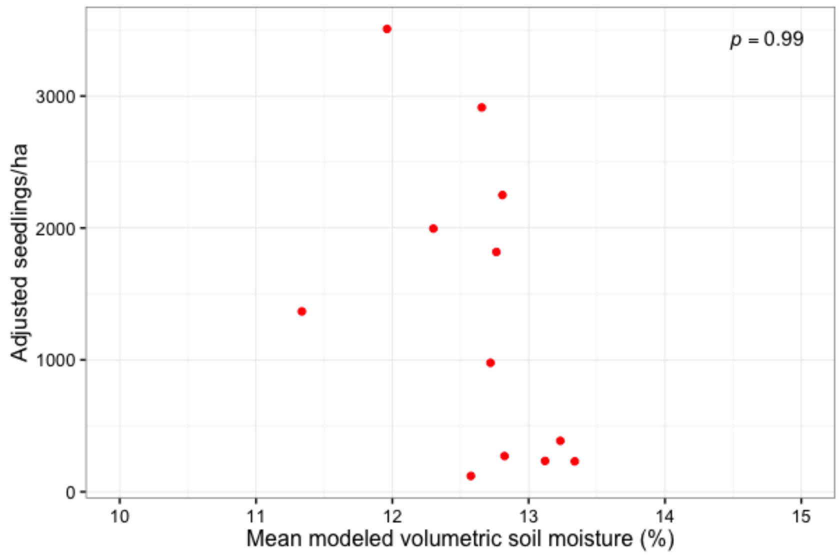

Figure 2.11. Seedling density as a function of average daily modeled soil moisture, expressed as a percentage of total saturation. P-value represents the result of an attempted linear regression.

In addition, I hypothesized that higher soil moisture during the early part of the growing season has a strong effect on the likelihood of seedling success. The VIC model output allowed me to test this hypothesis easily, in contrast to what would have likely been a very laborious and time-consuming field campaign. Thus I selected the first 45 days of the growing season to explore this idea and looked for a relationship between total moisture during that time period and seedling density. This metric had no significant relationship with seedling success (Fig. 2.12), nor did average moisture during that time period (not shown.)

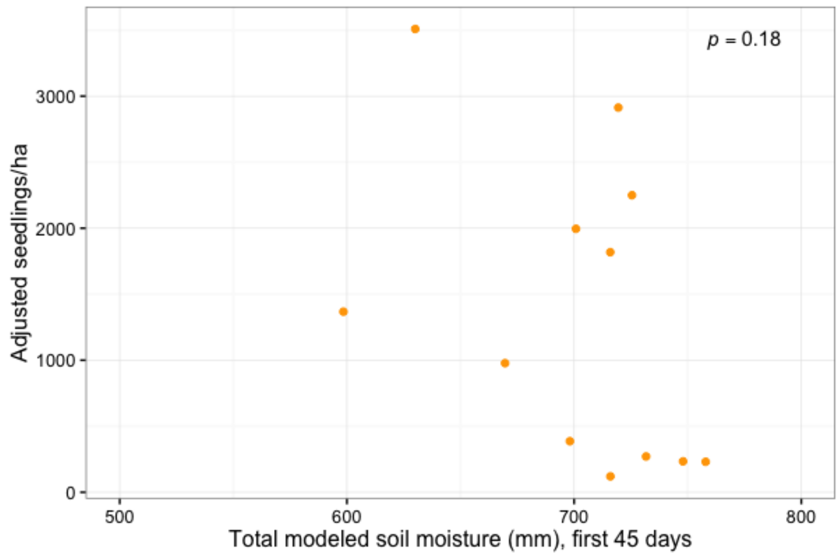

Figure 2.12. Adjusted seedling density as a function of total modeled soil moisture during the first 45 days of the VIC soil moisture output. P-value represents the result of an attempted linear regression.

I also hypothesized that the persistence of soil moisture in a given plot would create conditions more favorable to seedlings. Persistence provides a metric of how much moisture conditions persist, or stay similar over time. Given the importance of sufficient moisture for seedlings, I came to such a hypothesis based on the idea that longer periods of available moisture would predict greater likelihood of seedling success. To assess this, I used autocorrelation functions, a common method in time series analysis. The autocorrelation function calculates how similar any given data point along a time series is to the same data point a certain time period earlier, resulting in a final score representing a time series signal as a function of the specified time lag (Crawley, 2013). Using VIC model output, I calculated autocorrelation functions for monthly and weekly lags in soil moisture, as well as for weekly lag during the first 45 days of the growing season. The results show a significant ($p<0.05$) negative relationship between soil moisture persistence and seedling density (Figs. 2.13-2.15.)

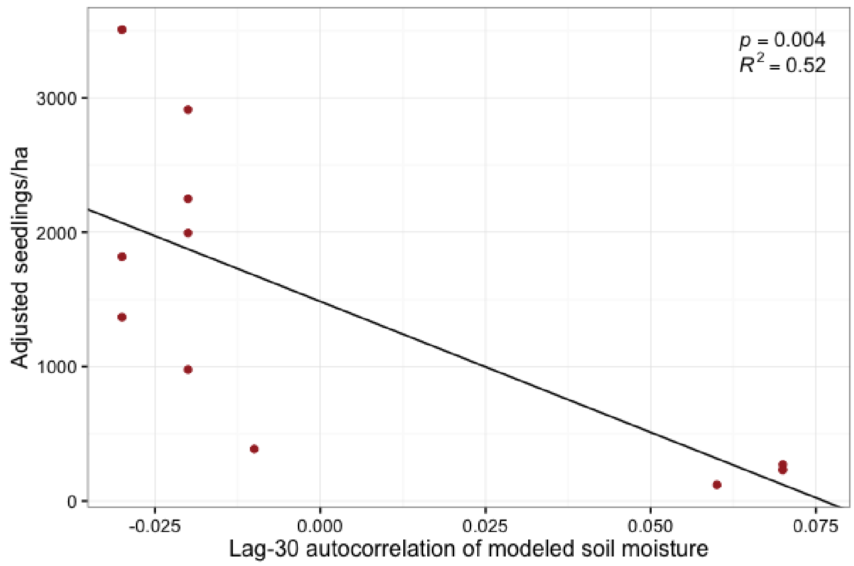

Figure 2.13. 30-day lag autocorrelation of VIC modeled growing season soil moisture predicts lower adjusted seedling density. Line, p-value, and R^2 represent results of a linear regression.

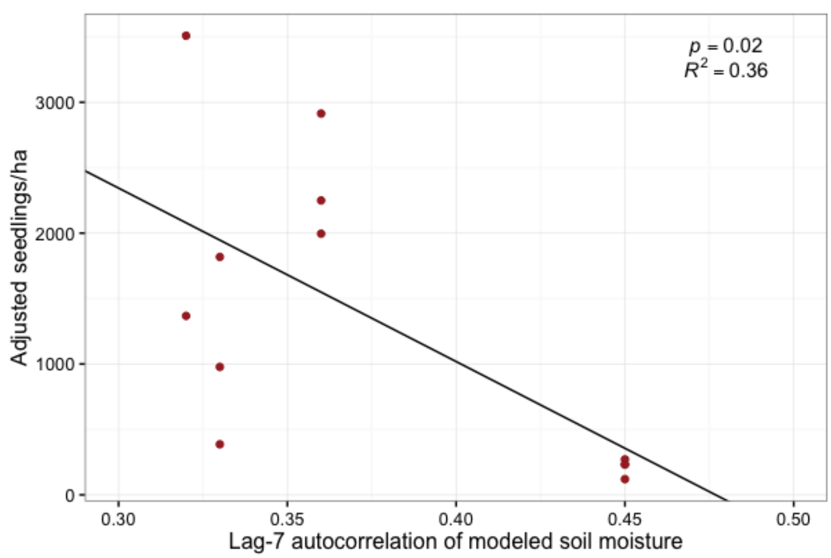

Figure 2.14. Same as Fig. 2.12, but 7-day lag autocorrelation of modeled soil moisture instead of 30-day lag.

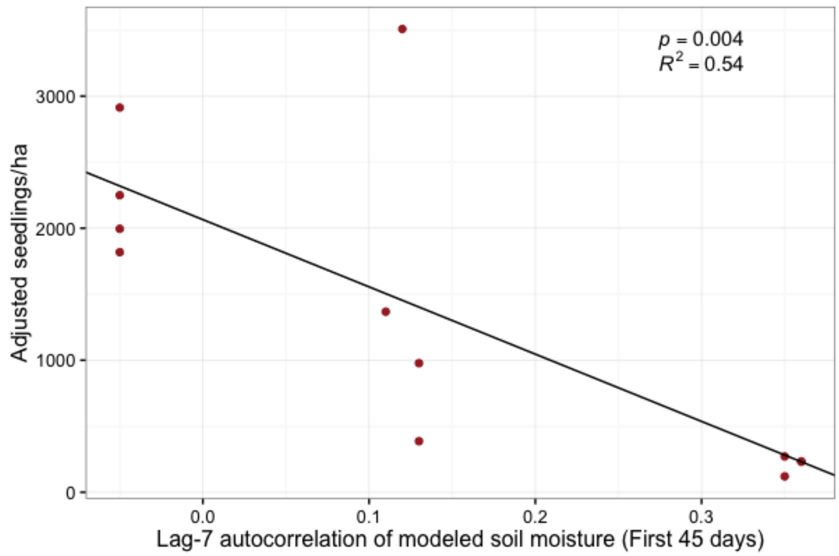

Figure 2.15. Same as Figure 2.13, but using only modeled soil moisture values for the first 45 days of the growing season.

Given that persistence of soil moisture had a negative relationship with seedling density, I then calculated kurtosis of modeled soil moisture to determine if it had predictive power. Kurtosis is a measure of the “peakedness” of a set of continuous data; in other words, it provides a single measurement of how quickly a variable rises and falls over time (Rogerson, 2006). Higher values of kurtosis, therefore, would indicate more rapid changes in soil moisture over the course of the growing season. As Figure 2.16 shows, kurtosis of modeled growing season soil moisture was indeed a significant predictor, explaining nearly 50 percent of the change in adjusted seedling density, according to a linear regression model.

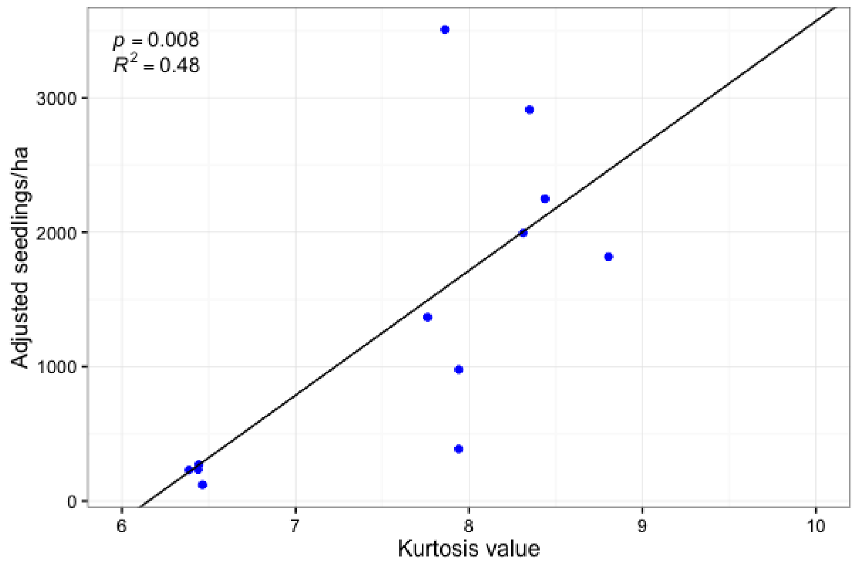

Figure 2.16. Adjusted seedling density as a function of kurtosis of modeled soil moisture. Line, p-value and R^2 represent the results of a linear regression.

Discussion

The results presented above are from a relatively small number of study plots established in the aftermath of a single wildfire. However, despite the lack of a larger data set, these analyses provide a starting point for further investigations that can draw upon the computational efficiency and scalability of the methods used here.

This thesis demonstrates that, after collecting a few plot characteristics and a relative handful of field measurements of soil moisture, the VIC model can be used to characterize soil moisture across heterogeneous landscapes. Given the flexibility of the model, it is wholly plausible that the scope of similar modeling efforts could cover a range of spatial scales. I was able to reproduce the general pattern of soil moisture decay over the course of the growing season and demonstrated responsiveness of soil moisture in the model to daily summertime precipitation events. More importantly, the model produced daily data and could be parameterized to produce sub-daily output given input data with appropriate time steps. The computational efficiency of the VIC model makes this an appealing approach for approximating soil moisture at the plot or larger scale, rather than relying on point-scale or plant-scale measurements as would be gathered by continuous field monitoring.

Given the demonstrated ability to reproduce soil moisture at the plot scale, the results of analyses of the relationship between soil moisture and seedling success merit further exploration. There is evidence that kurtosis of modeled growing season soil moisture is a promising metric for predicting likelihood of post-fire recovery by conifers at plot or landscape scales. This pushes beyond findings from the literature that demonstrate the importance of available moisture and vapor pressure deficit on the ability of a seedling to survive (e.g., Von Arx et al., 2013), implying that soils where moisture persists for too long could be less suitable and that repeated additions of soil moisture from episodic growing season precipitation may be more important than overall moisture availability, at least in subalpine forests recovering from recent wildfires. Additional field-calibrated moisture outputs and seedling counts from other post-fire sites are needed to build more evidence for the utility of soil moisture kurtosis as valuable metric.

From an ecological standpoint, this work raises additional questions about how the spatial distribution of land surface conditions affects recovery after wildfire. Ecophysiology research gives us good insight into plant-scale conditions affecting seedling survival during early succession after disturbance in subalpine forests and post-disturbance studies inform our understanding of general trajectories in structure and composition. However, we lack a clear understanding of the specific factors that control the direction of these trajectories at larger scales in heterogeneous landscapes. Moving further in that direction will require a combination of insights drawn from ecophysiology, ecohydrology, and landscape ecology using tools such as land surface modeling, spatial analyses, and field measurements.

Thus logical follow-up work building on this study would begin with a replication of the VIC modeling effort using field data from a number of other sites. Regardless of disturbance condition, the ability of the model to reproduce soil moisture conditions in heterogeneous, rocky soils found in the subalpine could be tested at multiple other sites, and the model could be better calibrated to improve representativeness of soil moisture. Following such an effort, the seedling study could be replicated at multiple other sites to assess whether the predictive power of kurtosis remains and whether other metrics, which were not significant predictors in this study, might still have a relationship to seedling success. Given the infrequency of fires in the subalpine zone (Baker, 2009), this may be a challenge, but incorporating field sites from across a wide area, such as the U.S. West, should provide sufficient replicates.

Finally, ecohydrologists and soil scientists may wish to further investigate questions related to better measurement and representation of soil moisture in rocky areas. Time domain reflectometry, used to obtain field measurements in this study, provides an efficient and cost-effective means to measure soil moisture but faces challenges in areas with very rocky soil. Moreover, the VIC model itself assumes soil heterogeneity. Those familiar with the model could investigate whether the pedotransfer functions in the model could be adjusted to better simulate rocky soils, or whether integration with another model could improve the quality of model output.

References

AghaKouchak, A., Berbery, H., Dong, J., Hoerling, M., Kumar, A., Lakshmi, V., Leung, R., Li, J., Liang, X., Luo, L., Lyon, B., Miskus, D., Mo, K., Quan, X., Schubert, S., Seager, R., Sorooshian, S., Wang, H., Xia, Y., Zeng, N., 2013. An Interpretation of the Origins of the 2012 Central Great Plains Drought.

Aussenac, G., 2000. Interactions between forest stands and microclimate: Ecophysiological aspects and consequences for silviculture. Ann. For. Sci. 57, 287–301. doi:10.1051/forest:2000119

Baker, W.L., 2009. Fire Ecology in Rocky Mountain Landscapes. Island Press, Washington, D.C.

Bigler, C., Kulakowski, D., Veblen, T.T., 2005. Multiple disturbance interactions and drought influence fire severity in rocky mountain subalpine forests. Ecology 86, 3018–3029. doi:10.1890/05-0011

Boone, R.D., Grigal, D.F., Sollins, P., Ahrens, R.J., Armstrong, D.E., 1999. Soil Sampling, Preparation, Archiving, and Quality Control, in: Robertson, G.P., Coleman, D.C., Bledsoe, C.S., Sollins, P. (Eds.), Standard Soil Methods for Long-Term Ecological Research. Oxford University Press, New York, NY, pp. 3–28.

Brady, N.C., 1974. The Nature and Properties of Soils. MacMillan Publishing Co., Ltd., New York, NY.

Buma, B., Wessman, C.A., 2012. Differential species responses to compounded perturbations and implications for landscape heterogeneity and resilience. For. Ecol. Manage. 266, 25–33. doi:10.1016/j.foreco.2011.10.040

Castro, J., 2016. Castro J , Zamora R , Hódar JA , Gómez JM . Seedling establishment of a boreal tree species (Pinus sylvestris) at its southernmost distribution limit : consequences of being in a margin ... Seedling establishment of a boreal tree species (Pinus sylvest 266–277. doi:10.1111/j.0022-0477.2004.00870.x

Collins, B.J., Rhoades, C.C., Battaglia, M.A., Hubbard, R.M., 2012. The effects of bark beetle outbreaks on forest development, fuel loads and potential fire behavior in salvage logged and untreated lodgepole pine forests. For. Ecol. Manage. 284, 260–268. doi:10.1016/j.foreco.2012.07.027

Collins, B.J., Rhoades, C.C., Hubbard, R.M., Battaglia, M.A., 2011. Tree regeneration and future stand development after bark beetle infestation and harvesting in Colorado lodgepole pine stands. For. Ecol. Manage. 261, 2168–2175. doi:10.1016/j.foreco.2011.03.016

Crawley, M.J., 2013. The R Book, 2nd ed. John Wiley & Sons, Ltd., West Sussex, UK.

Dennison, P.E., Brewer, S. c., Arnold, J.D., Moritz, M. a., 2014. Geophysical Research Letters. Geophys. Prospect. 41, 2928–2933. doi:10.1002/2014GL061184.Received

Elliott, E.T., Heil, J.W., Kelly, E.F., Monger, H.C., 1999. Soil Structural and Other Physical Properties, in: Robertson, G.P., Coleman, D.C., Bledsoe, C.S., Sollins, P. (Eds.), Standard Soil Methods for Long-Term Ecological Research. Oxford University Press, New York, NY, pp. 74–88.

Entekhabi, D., Njoku, E.G., O'Neill, P.E., Kellogg, K.H., Crow, W.T., Edelstein, W.N., Entin, J.K., Goodman, S.D., Jackson, T.J., Johnson, J., Kimball, J., Piepmeier, J.R., Koster, R.D., Martin, N., McDonald, K.C., Moghaddam, M., Moran, S., Reichle, R., Shi, J.C., Spencer, M.W., Thurman, S.W., Tsang, L., Van Zyl, J., 2010. The soil moisture active passive (SMAP) mission. Proc. IEEE 98, 704–716. doi:10.1109/JPROC.2010.2043918

Graham, R.T., Harvey, A.E., Jurgensen, M.F., Jain, T.B., Tonn, J.R., Page-dumroese, D.S., 1994. Managing Coarse Woody Debris in Forests of the Rocky Mountains. For. Sci. 12.

Gray, A., Zald, H., Kern, R., North, M., 2005. Stand conditions associated with tree regeneration in Sierran mixed conifer-forests. For. Sci 51, 198–210.

Jarrell, W.M., Armstrong, D.E., Grigal, D.F., Kelly, E.F., Monger, H.C., Wedin, D.A., 1999. Soil Water and Temperature Status, in: Robertson, G.P., Coleman, D.C., Bledsoe, C.S., Sollins, P. (Eds.), Standard Soil Methods for Long-Term Ecological Research. Oxford University Press, New York, NY, pp. 55–73.

Knapp, A.K., Smith, W.K., 1982. Factors influencing understory seedling establishment of Engelmann spruce (*Picea engelmannii*) and subalpine fir (*Abies lasiocarpa*) in southeast Wyoming. Can. J. Bot. 60, 2753–2761. doi:10.1139/b82-337

Kulakowski, D., Matthews, C., Jarvis, D., Veblen, T.T., 2013. Compounded disturbances in sub-alpine forests in western Colorado favour future dominance by quaking aspen (Populus tremuloides). J. Veg. Sci. 24, 168–176. doi:10.1111/j.1654-1103.2012.01437.x

Lajzerowicz, C.C., Walters, M.B., Krasowski, M., Massicotte, H.B., 2004. Light and temperature differentially colimit subalpine fir and Engelmann spruce seedling growth in partial-cut subalpine forests. Can. J. For. Res. 34, 249–260. doi:10.1139/x03-198

Liang, X., Lettenmaier, D.P., Wood, E.F., Burges, S.J., 1994. A simple hydrologically based model of land surface water and energy fluxes for general circulation models. J. Geophys. Res. 99, 14415. doi:10.1029/94JD00483

Livneh, B., Deems, J.S., Buma, B., Barsugli, J.J., Schneider, D., Molotch, N.P., Wolter, K., Wessman, C.A., 2015. Catchment response to bark beetle outbreak and dust-on-snow in the Colorado Rocky Mountains. J. Hydrol. 523, 196–210. doi:10.1016/j.jhydrol.2015.01.039

Miller, J.D., Knapp, E.E., Key, C.H., Skinner, C.N., Isbell, C.J., Creasy, R.M., Sherlock, J.W., 2009. Calibration and validation of the relative differenced Normalized Burn Ratio (RdNBR) to three measures of fire severity in the Sierra Nevada and Klamath Mountains, California, USA. Remote Sens. Environ. 113, 645–656. doi:10.1016/j.rse.2008.11.009

Oliver, C.D., Larson, B.C., 1990. Forest Stand Dynamics. The McGraw-Hill Companies, New

York, NY.

Painter, T.H., Rittger, K., McKenzie, C., Slaughter, P., Davis, R.E., Dozier, J., 2009. Retrieval of subpixel snow covered area, grain size, and albedo from MODIS. Remote Sens. Environ. 113, 868–879. doi:10.1016/j.rse.2009.01.001

Peet, R., 1981. Forest vegetation of the Colorado front range. Vegetatio 45, 3–75.

Pelz, K. a., Smith, F.W., 2012. Thirty year change in lodgepole and lodgepole/mixed conifer forest structure following 1980s mountain pine beetle outbreak in western Colorado, USA. For. Ecol. Manage. 280, 93–102. doi:10.1016/j.foreco.2012.05.032

Pugh, E., Gordon, E., 2013. A conceptual model of water yield effects from beetle-induced tree death in snow-dominated lodgepole pine forests. Hydrol. Process. 27, 2048–2060.

R Core Team, 2016. R: A Language and Environment for Statistical Computing.

Rogerson, P.A., 2006. Statistical Methods for Geography. Sage Publications, Ltd., Thousand Oaks, CA.

Singh, V.P., Woolhiser, D.A., 2002. Mathematical Modeling of Watershed Hydrology. J. Hydrol. Eng. 7, 270–292.

Soil Survey Staff, Natural Resources Conservation Service, U.S.D. of A., n.d. Web Soil Survey [WWW Document]. URL http://websoilsurvey.nrcs.usda.gov/ (accessed 4.10.16).

Turner, M.G., Gardner, R.H., O'Neill, R. V., 2011. Landscape Ecology in Theory and Practice. Springer-Verlag, New York, NY.

Ubeda, X., Outeiro, L.R., 2009. Physical and chemical effects of fire on soil, in: Fire Effects on Soils and Restoration Strategies. Science Publishers, Enfield, NH.

US National Park Service, n.d. Fern Lake Fire [WWW Document]. URL https://www.nps.gov/romo/learn/nature/fern_lake_fire.htm (accessed 10.1.16).

Veblen, T.T., Hadley, K.S., Reid, M.S., 1991. Disturbance and Stand Development of a Colorado Subalpine Forest. J. Biogeogr. 18, 707–716.

Von Arx, G., Graf Pannatier, E., Thimonier, A., Rebetez, M., 2013. Microclimate in forests with varying leaf area index and soil moisture: Potential implications for seedling establishment in a changing climate. J. Ecol. 101, 1201–1213. doi:10.1111/1365-2745.12121

Wu, J., 2013. Key concepts and research topics in landscape ecology revisited: 30 years after the Allerton Park workshop. Landsc. Ecol. 28, 1–11. doi:10.1007/s10980-012-9836-y